AD-A075 011 DAYTON UNIV OHIO F/G 6/19
A MODEL FOR THE ENERGETIC COST OF ACCELERATION STRESS PROTECTIO--ETC(U)
JUL 79 D B ROGERS F33615-78-C-0501
UNCLASSIFIED AMRL-TR-79-58 NL

| OF |
AD
A075011

END
DATE
FILMED
11-79
DDC

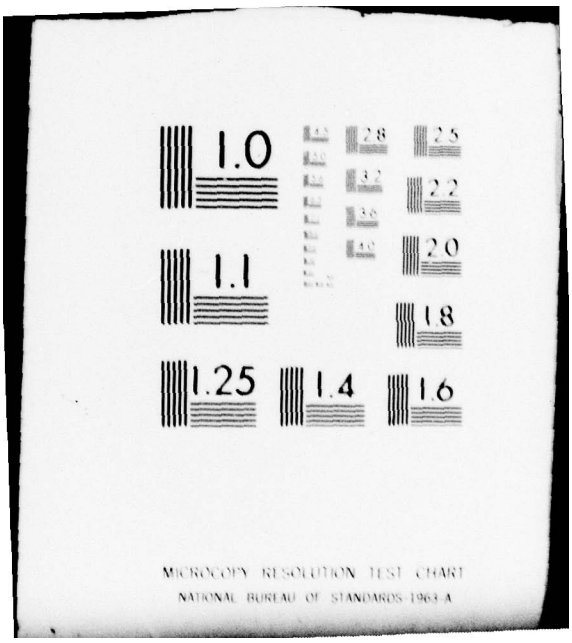
1.0
1.1
1.25
1.4
1.6
2.8
3.2
3.6
4.0
2.5
2.2
2.0
1.8
MICROCOPY RESOLUTION TEST CHART
NATIONAL BUREAU OF STANDARDS-1963-A

AMRL-TR-79-58

LEVEL II

A MODEL FOR THE ENERGETIC COST OF ACCELERATION STRESS PROTECTION IN THE HUMAN

DANA B. ROGERS, Ph.D.

UNIVERSITY OF NEW HAMPSHIRE
COLLEGE OF ENGINEERING AND PHYSICAL SCIENCES
DURHAM, NEW HAMPSHIRE 03824

JULY 1979

Approved for public release; distribution unlimited.

AEROSPACE MEDICAL RESEARCH LABORATORY
AEROSPACE MEDICAL DIVISION
AIR FORCE SYSTEMS COMMAND
WRIGHT-PATTERSON AIR FORCE BASE, OHIO 45433

NOTICES

When US Government drawings, specifications, or other data are used for any purpose other than a definitely related Government procurement operation, the Government thereby incurs no responsibility nor any obligation whatsoever, and the fact that the Government may have formulated, furnished, or in any way supplied the said drawings, specifications, or other data, is not to be regarded by implication or otherwise, as in any manner licensing the holder or any other person or corporation, or conveying any rights or permission to manufacture, use, or sell any patented invention that may in any way be related thereto.

Please do not request copies of this report from Aerospace Medical Research Laboratory. Additional copies may be purchased from:

National Technical Information Service
5285 Port Royal Road
Springfield, Virginia 22161

Federal Government agencies and their contractors registered with Defense Documentation Center should direct requests for copies of this report to:

Defense Documentation Center
Cameron Station
Alexandria, Virginia 22314

TECHNICAL REVIEW AND APPROVAL

AMRL-TR-79-58

This report has been reviewed by the Information Office (OI) and is releasable to the National Technical Information Service (NTIS). At NTIS, it will be available to the general public, including foreign nations.

This technical report has been reviewed and is approved for publication.

FOR THE COMMANDER

ENSOR RODRIGUEZ-LOPEZ, Colonel, USAF, MC
Acting Chief,
Manned Systems Effectiveness Division
Aerospace Medical Research Laboratory

AIR FORCE/56780/5 September 1979 — 150

(18) AMRL, AMRL

SECURITY CLASSIFICATION OF THIS PAGE *(When Data Entered)*

(19) **REPORT DOCUMENTATION PAGE**

READ INSTRUCTIONS BEFORE COMPLETING FORM

1. REPORT NUMBER: AMRL-TR-79-58, LDF-78-5 (9)	2. GOVT ACCESSION NO. / 3. RECIPIENT'S CATALOG NUMBER: Final
4. TITLE *(and Subtitle)*: (6) A MODEL FOR THE ENERGETIC COST OF ACCELERATION STRESS PROTECTION IN THE HUMAN.	5. TYPE OF REPORT & PERIOD COVERED: Technical Report. 1 Jan 1978 — 31 May 1979
	6. PERFORMING ORG. REPORT NUMBER: LDF78-5
7. AUTHOR(s): (10) Dana B. Rogers, Ph.D.	8. CONTRACT OR GRANT NUMBER(s): (15) F33615-78-C-0501
9. PERFORMING ORGANIZATION NAME AND ADDRESS: University of New Hampshire, College of Engineering and Physical Sciences, Durham, New Hampshire 03824	10. PROGRAM ELEMENT, PROJECT, TASK AREA & WORK UNIT NUMBERS: (16) (17) 62202F 6893 07 03
11. CONTROLLING OFFICE NAME AND ADDRESS: Aerospace Medical Research Laboratory, Aerospace Medical Division, Air Force Systems Command, Wright-Patterson Air Force Base, Ohio 45433	12. REPORT DATE: (11) July 1979 / 13. NUMBER OF PAGES: 60
14. MONITORING AGENCY NAME & ADDRESS *(if different from Controlling Office)*: (12) 60	15. SECURITY CLASS. *(of this report)*: Unclassified / 15a. DECLASSIFICATION/DOWNGRADING SCHEDULE

16. DISTRIBUTION STATEMENT *(of this Report)*

Approved for public release; distribution unlimited.

17. DISTRIBUTION STATEMENT *(of the abstract entered in Block 20, if different from Report)*

18. SUPPLEMENTARY NOTES

19. KEY WORDS *(Continue on reverse side if necessary and identify by block number)*

Acceleration
Stress
Cardiovascular
Energetics
Protection
Performance

20. ABSTRACT *(Continue on reverse side if necessary and identify by block number)*

Dynamic models of selected portions of the human physiology are developed and integrated as a general model of the human response to sustained acceleration. Each model is developed to represent the physiologic response and still retain structural identifiability. The assembled and separate models provide a means for exploring various mission profiles. The model provides insights into the problems inherent in the dynamic application of the protection strategies involved in optimizing mans performance in high agility aircraft.

DD FORM 1 JAN 73 1473 EDITION OF 1 NOV 65 IS OBSOLETE

SECURITY CLASSIFICATION OF THIS PAGE *(When Data Entered)*

195 350

SUMMARY

Increased gravitational force stresses the human physiology in a manner that causes detrimental changes in the human's capability to maintain acceptable performance levels. A set of physiologic models which dynamically describe acceleration stress responses are developed in this report. Each of the models represents a major physiologic system or acceleration protection mechanism. The submodels are assembled as a larger system using natural linkage variables from one subsystem to the next. The major subsystems are the Visual System, Cardiovascular subsystem, G suit system, Straining system, Decision system and the Energy Cost System. Each model is developed to the extent possible based on current knowledge.

The use of dynamic models, presented as separate systems allows for a variety of speculative studies. A system model assembly which emphasises the optimal expenditure of energy by the human in conjunction with his protective equipment, demonstrates the tradeoff necessary between peak G capability vs the energetic cost to withstand sustained acceleration at the peak level. The model demonstrates the need to establish an effort strategy which will utilize the available physiologic energy in an efficient manner. The separate submodels provide a means of evaluating the major subsystem responses to the acceleration stressor in a dynamic fashion. The model further provides the basis for redefinition and extension of acceleration research into familiar areas with new intent.

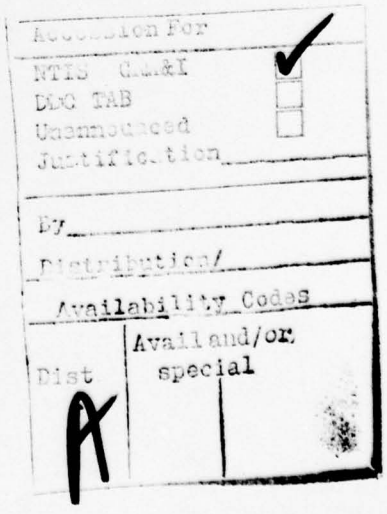

PREFACE

This final report was prepared by the Department of Electrical Engineering University of New Hampshire under Contract F33615-78-C-0501 with the Aerospace Medical Research Laboratory (AMRL). The program was under the technical direction of Dr. James Veghte of the Human Operator Performance Branch, Manned-Systems Effectiveness Division, AMRL. Funding was provided by the Laboratory Director's Funds, LDF-78-5.

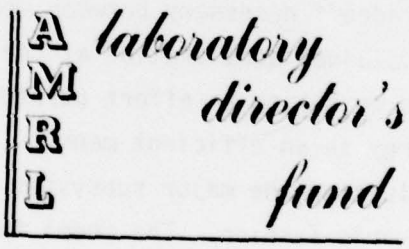

TABLE OF CONTENTS

LIST OF FIGURES

SECTION 1

INTRODUCTION

Background

Increased gravitational force results in a number of physiologic changes in the human exposed to such an acceleration. Classical methods of measuring these effects have led to an ever increasing knowledge of the stressed physiologic systems (5). The two systems which have classically provided the defining limits in the stressed condition are vision and fatique which then impinge on the performance capabilities of the human. Various performance measures have also been used to develop a greater knowledge of the acceleration environment. A multitude of model structures have arisen to describe the changes in oxygen levels blood pressure, and in visual capability in hope of providing better descriptions and directions for advanced research. The model in this report has been developed from an alternative standpoint. The supposition is that there are competing systems within the human physiology which require oxygen, in order to function at an acceptable level. The visual system requires a continuous flow of oxygen to the retinal layer to maintain function. The muscle system requires oxygen for replenishment of anaerobic activity and supply for aerobic activity. The central nervous system requires the same oxygen for its sustained higher level activity. The model in this development then becomes a model related to oxygen transport and competing energy used in the stressed physiologic system.

A set of submodels are developed based on these energetic requirements. The resulting model integration allows investigation of the model in terms of an optimally controlled system. For example, varying acceleration time profiles can be run on the model with energy cost or acceleration level cost functions having the greater weight. Performance is included through the pattern analysis inherent in the visual modulation transfer function and the cerebral oxygenation prediction. The system model provides the basis for redefinition and extension of acceleration research into familiar areas with new intent.

Physiologic Factors of Acceleration Tolerance

The physiologic changes caused by acceleration have been reported extensively in research literature (5, 16). The two widely recognized factors

which contribute to pilot impairment in maneuvering aircraft are fatigue and visual dimming. These two factors can be included in a simulation model system to enhance the reality of simulated air combat. The visual system is directly affected by the ability of the cardiovascular system to deliver adequate blood pressure to the eye. Vision for the pilot is impaired as the retina responds to acceleration induced changes in the eye level blood pressure. Experimentation shows that the cardiovascular system has a well defined relaxed G limit above which visual integrity cannot be maintained without the addition of energy consuming maneuvers of straining and muscle tensing. Thus, the energy cost to a subject in maintaining visual function at the G level above his natural relaxed G_z limit is greater than the energy cost at a lower G level. At some level of energy expenditure there is a maximum limit above which the subject cannot maintain vision regardless of straining energy used.

The cardiovascular system has received the greatest attention in acceleration stress studies as it provides an easily measured set of parameters. The limiting factor in the cardiovascular system, from the viewpoint of combat maneuvering stress, is the reduction of blood pressure at eye level and subsequent loss of vision. The pressure gradient changes caused by the G loading and blood pooling are, of course, the major contributing factors which reduce the pressure available at the eye and in more severe cases at the brain. Counteracting the reduced pressure is the primary purpose of straining maneuvers (M-1 and L-1, Appendix A). Blood pooling in the lower body is reduced by use of the G-suit. The factors, then, which define an operating limit in the cardiovascular system, are related directly to the blood pressure response characteristics in the 3-15 second time frame (15). A composite of experimental results depicting acceleration tolerance end points is shown in Figure 1 (8, 17, 25). In general, the blood pressure response in a hypothetical acceleration field with 5G/sec onset shows a gradual decrease below baseline until eight seconds then a gradual increase to a final level still below baseline. The pressure receptors in the carotid sinus are the primary cause of this reflex action (38).

Another area of interest in the physiologic response to G stress is the time period beyond 15 seconds. Once the pilot has passed a G stress level which represents his/her relaxed tolerance [energy must be expended] in straining to increase blood pressure and thus maintain vision. The amount of energy expended in the blood pressure maintenance task is a factor of the straining

efficiency and the magnitude of the G difference between the relaxed tolerance and the current G stress level. It can be speculated that the time endurance limit is determined by the amount of straining energy used in visual maintenance. When the energy pool is diminished to a certain level the fatigue limit is reached.

The Pulmonary circulation is also a critical factor in determining the amount of oxygen available to the physiologic system. Acceleration stress causes a reduced blood flow to the ventilated areas of the lung which in turn reduces the arterial oxygen concentration, Glaister (21). Therefore there is a concomitant reduction in the oxygen delivery from the external environment.

The system model is shown in Figure 2. The model rationale is that of energy balance or oxygen balance and provides a rational basis for description of previously recorded experimental evidence. The model also generates a new set of questions and requires a new set of experimental evidence in certain areas to establish a validation from the new viewpoint. The transition from oxygen depletion to CNS impairment and acceleration levels to manipulative control models is left to others.

Each of the computer based models is derived from literature and/or experimentation and each subsection represents a partition of the complex system into more easily modeled subsystems.

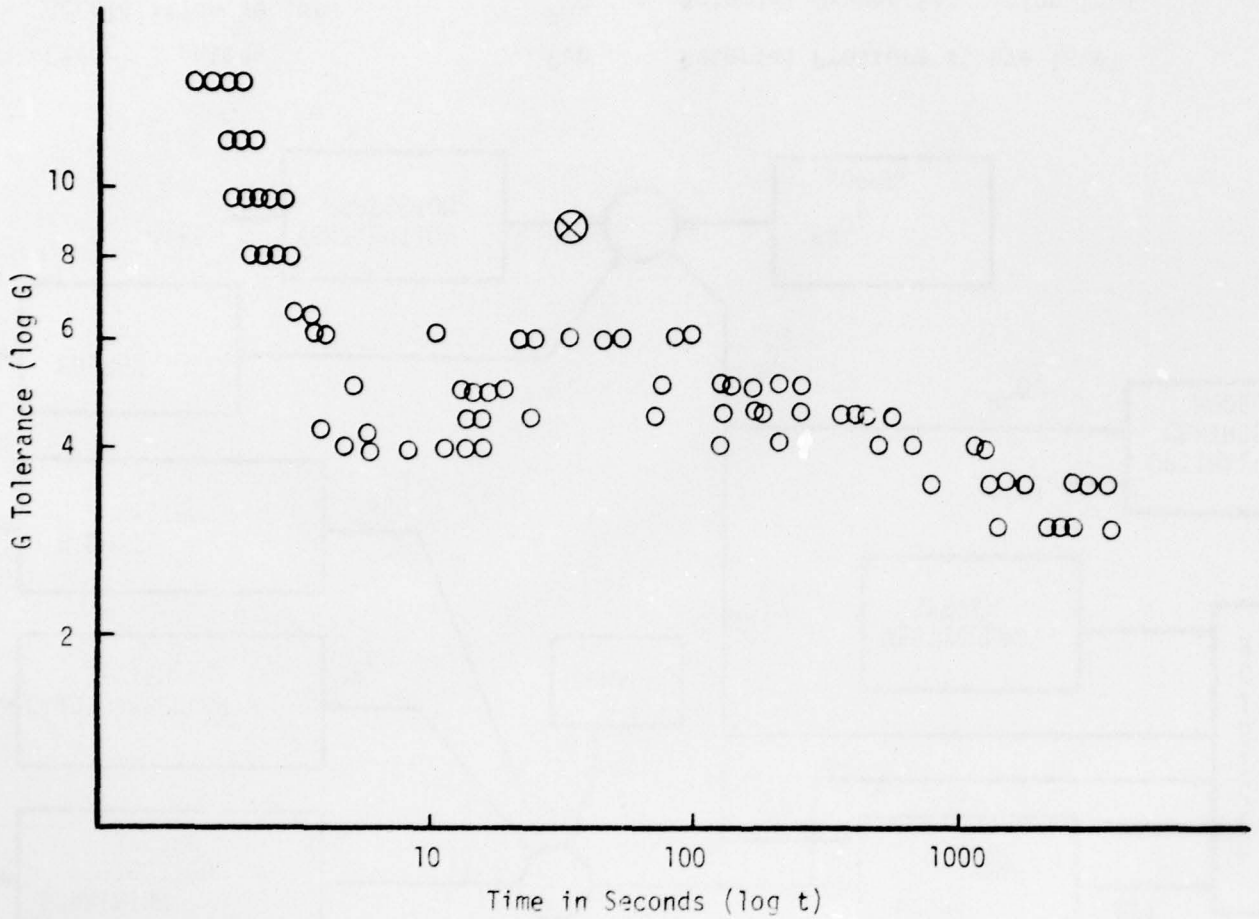

Figure 1. Composite G Tolerance Time Plot
⊗ 9 of 14 subjects at 9G for 45 seconds
O Acceleration tolerance for single subjects (8, 17, 26)

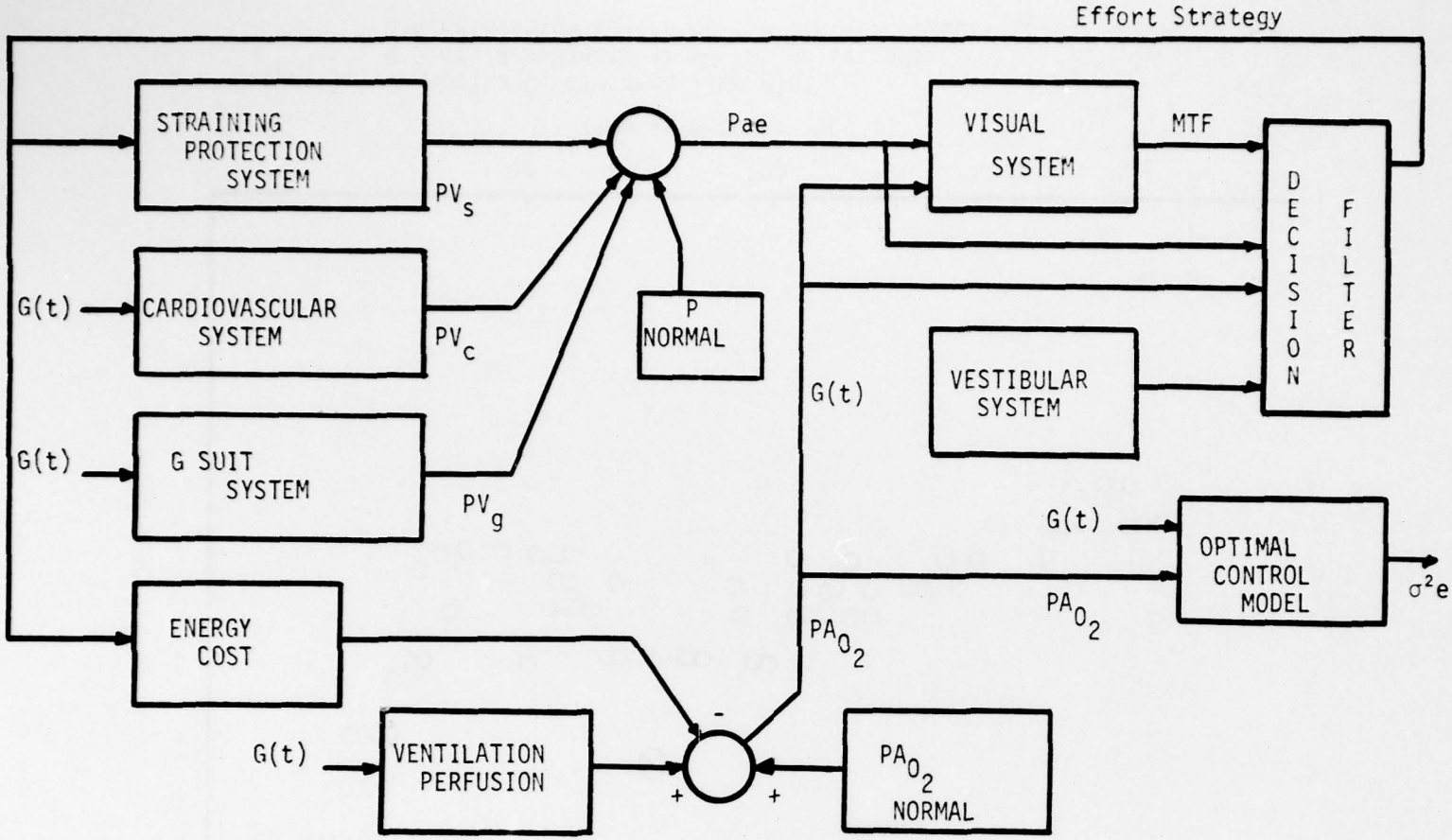

LEGEND

E(t) = Effort Strategy

G(t) = Acceleration Vector

PVs = Protection Value of Straining

PVc = Protection Value of Cardiovascular

PVg = Protection Value of G Suit

Pae = Arterial Pressure at eye level

PA_{O_2} = Arterial Oxygen Saturation in %

$\sigma^2 e$ = General Performance Metric

MTF = Modulation Transfer Function

Figure 2. Energetic System Model for Acceleration Stress/Performance

SECTION 2

THE PHYSIOLOGIC MODELS

Introduction

The human organism is a highly complex system of interconnecting and interdependent systems. Linearization of any of these systems is a precarious practice if the attempt is to define the total system. However by restricting the modeling effort to the problem at hand some success can be immediately forthcoming. In attempting to tie the simulation of machines in direct connection with the man further allowances and restrictions are forced upon the modeler. Training and research simulation has an overriding requirement that the system must run in real time. Using the engineer's tools such as linear systems analysis, complex structural modeling and applying simplifying assumptions it is possible to define a manageable structure with some common signal set which relates each part of the model. The rationale behind this system structure is directed by such constraints.

The simulation submodels are selected by a partitioning process which separates identifiable physiologic systems. The systems are then modeled using a common dimensional signal as the output.

The integrated system is represented in Figure 2. The various model partitions are evident in the block diagram structure.

The Cardiovascular Response Model is represented by a dynamic linear transfer function which corresponds to the effect of acceleration on the pilot's blood pressure. One prime governing factor in pilot response to acceleration is the onset of greyout and blackout. These visual problems are directly related to the available blood pressure at eye level. This model output provides a dynamically responding signal which is equivalent to nominal eye level blood pressure values for an unprotected human undergoing the equivalent acceleration, G(t), profile.

The Straining Simulation Model accounts for the G tolerance enhancement which is afforded by a properly executed M-1 or L-1 maneuver. The purpose of these straining maneuvers is to increase the blood pressure delivered to the eye. Proper performance of the maneuvers requires that the abdominal and upper torso muscles be tensed isometrically and that expirations should be made against a partially closed or closed glottis. The result is an increased intrathoracic pressure and increased blood pressure at the eye. Proper

application of the straining maneuvers also results in the appearance of myoelectric signals (EMG) on the skin surface. These biologically derived signals may provide for an evaluation of the straining protection variable which represents the increased blood pressure due to the M-1 or L-1.

The Ventilation Perfusion Model allows the effects of reduced perfusion to be incorporated. Acceleration induced shifts in the pulmonary blood supply reduce the amount of oxygen transport across the alveolar surface and thus reduce the oxygen supply.

The results of oxygen/energy use in straining and the impaired supply through the ventilation perfusion changes are embodied in the energy stores Model.

The G Suit Model provides the parameters which describe the valve system and the garment used to increase the individuals tolerance to $+G_z$. The suit uses pressurized bladders to press against the legs and lower abdomen. The external pressure inhibits displacement of the blood volume to the lower extremities thus insuring a better blood supply to the heart during acceleration. The suit must be inflated by the G valve to a predetermined level for the suit to be effective. The simulation model accounts for the required pressure level and uses the actual suit to provide the necessary dynamics. The suit pressure is compared with the required schedule and a protection value is generated by the model.

The Dynamic Visual Field Model reacts to G level inputs from an external source and produces a dynamically responsive signal which predicts the expected visual field of a pilot undergoing the identical G profile.

The system presented on the following pages represents the results of partitioning the complex physiologic system into submodels. Each submodel is explored and developed in detail based on a common protection variable (PV) which is related physiologically to systemic blood pressure. The blood pressure models are then finally combined in a systematic paradigm which provides the driving values for the visual field response model.

The Cardiovascular Response Model

Background

Human tolerance to long term $+G_z$ acceleration is normally measured in terms of visual loss (blackout) and unconsciousness. Both of these tolerance end points are related to the ability of the cardiovascular system to deliver

oxygenated blood at adequate pressure to the retinal and cerebral regions. The acceleration causes a changing blood pressure profile in the human such that the effective pressure vertically above heart level is decreased and the pressure below heart level is increased. There is therefore a lower perfusion pressure at eye level. The distribution of the blood in the body also changes as the acceleration pools blood in the lower parts of the body and lungs. There is therefore less available blood to circulate and a lower oxygen content because the lungs do not operate as efficiently.

There are two cardiovascular systems which are dynamically involved in blood pressure maintenance which the human is undergoing $+G_z$ acceleration. The hydrostatic system which is related to classical fluid mechanics is responsible for the reduced retinal perfusion pressure at the eye and eventual loss of pressure at the cerebral level. The orthostatic system is related to blood pooling in the lower body with a concomitant reduction to venous return to the heart.

The cardiovascular system has self regulatory feedback systems which are affected by blood volume and pressure. The feedback systems attempt to regulate the pressure and flow characteristics of the cardiovascular system. One of the primary pressure sensors for this system is located in the carotid artery. Any change in pressure at the sensors results in a regulatory operation which attempts to return the pressure to a preset value. For example, a pressure drop at the carotid sinus initiates a neurologic reflex action which changes the heart rate and output so as to increase the overall pressure level. This section derives the rationale for a cardiovascular transfer function model which describes the G_z acceleration response of the blood pressure delivery system.

A radically new model for the cardiovascular system is not the intent of this study. Rather a reasonably accurate transfer function based on physiologic and physical principles as well as experimental observation is sought. The major requirements are that the transfer function model retain the major response characteristics of the cardiovascular system, be implementable in a real time digital simulation system, and retain factors which are identifiable with measurable physiologic factors.

Transfer Function Dynamics

Models of the cardiovascular system have been developed by investigators

(19, 30, 32, 45) in an attempt to better understand the underlying mechanisms which characterize the dynamic response of the system. The primary areas of investigation deal with the carotid sinus feedback reflex, peripheral resistance and blood distribution. Both animal analogs (principally canine) and human experimentation have led to the current knowledge about the blood pressure response to $+G_z$.

Canine blood pressure response curves have been derived by Knapp (30) with maximum gain in the 30 to 60 mHz range. Koushanpour, et al (32) show a first order transfer function with a 20 second time constant. Levison (38) has proposed a second order system for the canine carotid reflex with a natural frequence of 42 mHz. According to Scher (50) an adequate description of the pressure response transfer function can be made as a single zero double pole system. Gillingham (19) uses a single zero double pole system as one of his empirical functions. Examination of Gillingham's data as a Bode plot indicates that a single zero double pole transfer function can be applied with reasonable results. This study has adopted a similar function to represent the pressure-G_z acceleration (P-G) transfer function. The frequency range of interest is restricted to f = 200 mHz as the physiologic response of interest as long term maneuvering accelerations falls within this range. The generalized transfer function is:

$$P(s) = \frac{K_1(1 + a_1 s)}{1 + b_1 s + b_2 s^2} \qquad (1)$$

Values are selected for a_1, b_1, and b_2 as compromise values from the literature and Gillingham's response curves. The system lead term is selected at f_z = 30 mHz and the system response is selected as a complex pole at fp = 70 mHz and ξ = 0.7. For these breakpoints the values are a_1 = 5.31, b_1 = 3.23, and b_2 = 5.17 ($n_i = \frac{1}{2\pi f_z}$). The system gain k_1 is derived in the following section.

System Gain Derivation

The calculation of system gain requires the consideration of the laws of hydrostatics, anatomy and experimental observation. The occurrence of blackout defines the point at which blood pressure in the eye has dropped below some critical value. The difference between this critical value and the normal eye level pressure provides the basis for calculation of the linear gain value.

The resultant gain K_1 represents the static pressure loss at eye level per unit G_z under the assumption of constant pressure at the aortic arch.

The laws of hydrostatics requires that ideal fluids at rest under gravity have equal pressure in all directions at a point, have the same pressure at all points on equal gravity planes and that pressure varies with depth. In a gravity free environment the blood pressure would generally be constant over all areas of the body. Under this condition the effective internal eye level blood pressure would be 90 mm Hg assuming a 20 mm Hg intraocular pressure and a nominal systolic pressure of 110 mm Hg. If the body is placed in an acceleration environment the hydraulic column of the blood supply will take on differing pressures at different vertical distances as measured along the acceleration vector. The change in pressure due to acceleration and the hydraulic column is given by Pascal's Law of hydrostatic differences. This can be stated as the pressure at any point in a fluid with respect to another point is given by ρ Gh where ρ is the density of the liquid, G is the acceleration and h is the vertical distance to the reference point. The pressure in mm Hg at eye level is calculated as:

$$Pae = Pa - 0.77\ G(t)\ he \qquad (2)$$

where 0.77 is a conversion factor related to blood density with units of mm Hg/cm.

There is generally some angular displacement from vertical of the hydrostatic column between the aortic arch and the retina. This offset angle (θ) accounts for the G_z component of the acceleration vector. The pressure at heart level is given as Pa and the pressure at eye level is given as Pae. The hydraulic gain for the transfer function relating pressure at eye level to the acceleration level is then given by:

$$Pae - Pa = -0.77\ he \cos \theta / G \qquad (3)$$

The transfer function gain is:

$$K_1(\theta) = \frac{Pae - Pa}{G} = -0.77\ he \cos \theta \qquad (4)$$

For a nominal eye to aortic arch distance of 28 cm and $\theta = 0°$ the gain $K_1(\theta)$ is:

$$K_1(\theta) = -0.77\ (28)(1) = -21.6 \text{ mm Hg/G} \quad (5)$$

The gain value can also be calculated from blackout tolerance values derived from experiment. The blackout tolerance figure for unprotected subjects is reported by Burton (5) as 3.7 G_z+ .10 for peripheral light loss and as 4.7 G_z+ .8 for central light loss. The occurrence of central light loss or blackout corresponds to the cessation of blood flow through the retinal artery and therefore is the point at which the effective pressure has dropped to zero.

The effective retinal pressure is calculated as the difference between eye level blood pressure and the intraocular pressure (vide infra) where the intraocular pressure is chosen with a nominal value of 18 mm Hg (11).

$$P_R = Pae - 18 \text{ (mm Hg)} \quad (6)$$

$$(Pae = 120 - 0.77\ (30)1) \quad (7)$$

$$= 97 - 18 \text{ (mm Hg)} \quad (8)$$

$$= +79 \text{ mm Hg} \quad (9)$$

The G difference is taken from experiment (5) so that $K_1(\theta)$ is calculated as:

$$K_1(\theta) = \frac{79}{1 - 4.7} = -21.4 \text{ mm Hg/G} \quad (10)$$

The general transfer function is constructed using the derived values as shown in Figure 3.

The Protective Garmet Model (G Suit)

Background

The history of G-suits dates from World War II and has been reviewed in recent monographs (5, 15, 16, 29). The wrap-around CSU-3/P cutaway-type of anti-G suit, presently used by the U.S. Air Force, improves tolerance in the $+G_z$ vector by about $2+G_z$ (37). The protection effect of anti-G suits was originally established on the Toronto centrifuge and at the Mayo Clinic and has been summarized by Wood and Lambert (58). These studies showed that inflation of a G-suit at 1 G produces an initial increase in arterial pressure, followed

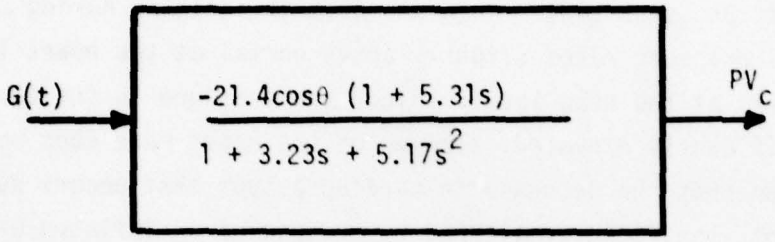

LEGEND

G(t)	=	Acceleration Vector
PV_c	=	Cardiovascular Protection Valve
s	=	Complex frequency

Figure 3. Block Diagram Model of Cardiovascular System Response

by an almost immediate decrease in heart rate probably due to a depressor reflex originating in the carotid sinus and aortic areas. Lindberg has observed that inflation of an anti-G suit under $+G_z$ acceleration is associated with a relative increase in mean aortic pressure which acts to counteract the increased hydrostatic pressure (43). When the suit is inflated during acceleration, the arterial pressure rises slightly above normal at the heart level but remains below normal at the head level. Since the pressure in the carotid sinus is not significantly elevated, slowing of the heart rate does not occur. Lindberg, has shown that the decrease in cardiac output that occurs during $+G_z$ acceleration is not significantly altered by the use of an inflated G-suit (43). Hence, the protection afforded by the suit is not associated with a relative increase in cardiac output.

McCally has shown that the G suit does not provide protection unless the suit is inflated to at least 80 mm Hg (46). In effect the pressure difference between the suit bladder and the hydrostatic blood pressure in the lower body must be such that the suit pressure is greater to effect a protection function. The same reasoning is used in developing the simulation model. The suit pressure must be within acceptable pressure tolerance or it will affort no protection value.

The G Suit Model

The protective G suit garmet contains airtight bladders which are filled with pressurized air delivered from a G sensitive mechanical valve. The pressure delivered by the valve is a function of the current G level. The normal suit pressure G relationship curve is presented in Figure 4.

At the lower end (left side of Figure 4) of the G-pressure curve it can be seen that G suit inflation does not begin until the valve has reached a level of 1.5-1.7 G. After this point the pressure output is a linear function of G with a value of approximately 75 mm Hg per G. The air bladders, the suit air feed hose and the containing garment represent a dead space which introduces a time delay into the pressure system. The delayed suit filling is caused by both a transport delay and first order lag. The transport time is caused by the connecting air feed line from valve to suit and is on the order of 5 msec. The bladder size and garmet tightness govern the lag term which has a time constant on the order of 1 sec. These relationships can be seen in Figures 5a and 5b.

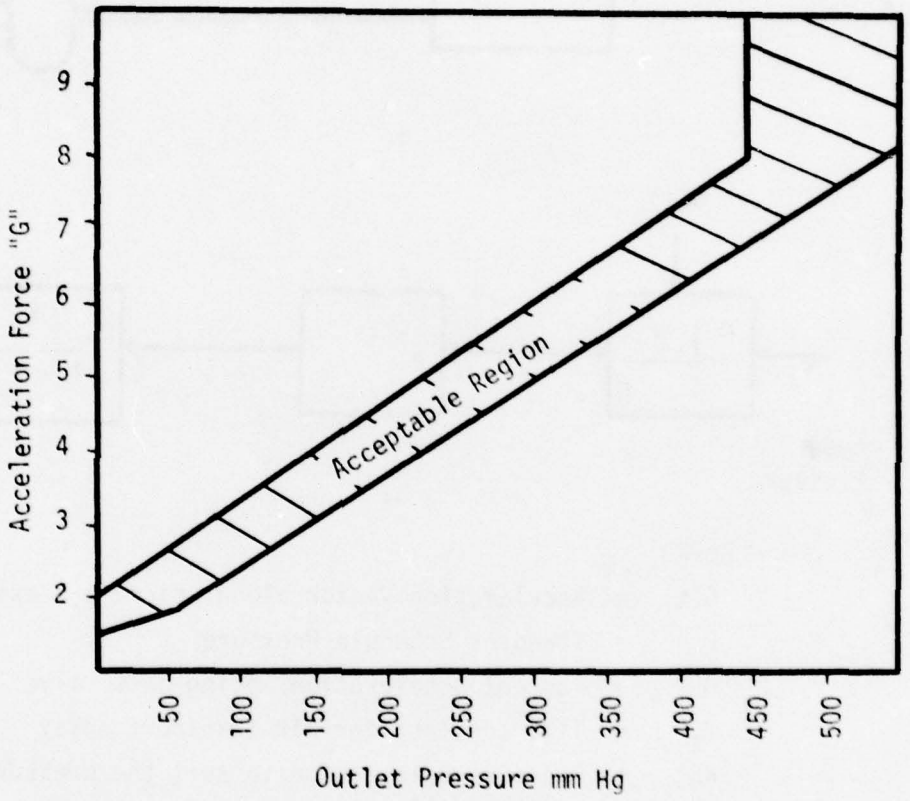

Figure 4. Standard Pressure Suit-Valve Fill Schedule

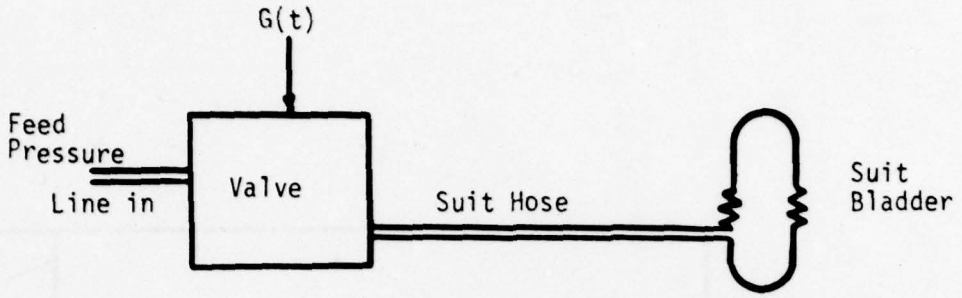

a.

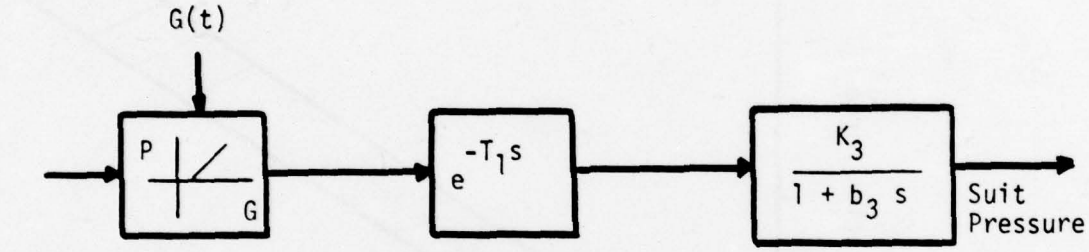

b.

LEGEND

G(t)	=	Acceleration Vector along aricraft z axis
P	=	Standard Schedule Pressure
G	=	Current Acceleration acting on G valve
T_1	=	Time constant for air transport delay
K_3	=	Pressure Gain inside to suit the pressure applied to skin
b_3	=	Time constant for air pressure fill lag time
s	=	Complex frequency

Figure 5. Simplified G Suit Pressure System Characteristics

In terms of the model, the dynamic G suit effects do not easily fit into the scheme of the blood pressure dependant variable. This must be circumvented in the integration of the system to allow for straightforward implementation. The general plan will be to establish a binary decision on appropriate suit pressure.

A blood pressure G suit model is chosen based on experimental values from MCally (46). The model assumes a nominal 2 G or equivalent 42.8 mm Hg increase for a properly inflated suit. For a suit with lower than designated pressure the increased G protection and equivalent blood pressure value decay linearly to 0. The model is driven by a delta P (ΔP_G) representing the pressure difference between the standard suit pressure curve and the actual suit pressure. When suit pressure is equal to or greater than the standard curve value, full protection is assumed. When the suit pressure is less than required by the standard curve, the protection value is lowered. When the pressure differential is greater than 80 mm Hg with the suit pressure below required values, there is no protection afforded by the simulation model.

$$\begin{aligned}
&\text{Where } \Delta P_G = \text{Suit Pressure - Standard Curve Pressure} \\
&\text{For } \quad \Delta P_G < -80 \text{ ——— Protection Value (PV) } 0 \\
&\text{For } -80 \leq \Delta P_G < 0 \text{ ——— } PV = \left(\frac{42.8}{80}\right)\Delta P + 42.8 \\
&\text{For } 0 \leq \Delta P_G \text{ ——— } PV = 42.8
\end{aligned} \tag{11}$$

It is most appropriate to include both suit dynamics and the physiologic system dynamics in the model. In fact the suit dynamics are included as a real time system by the implementation of the actual suit system pressure signal in the model. It is not possible to add the physiologic system dynamics at this time without greater definition of the protective mechanisms. However the errors inherent in the current system will not be of such magnitude that their effect will be noticeable in this simulation system. The suit dynamic effects may change the cardiovascular system transfer function. Both the stiffness of the system and the lead term of the G-P transfer function would probably be modified in a manner which cannot be accurately modelled. The simulation model is presented in block diagram form as Figure 6.

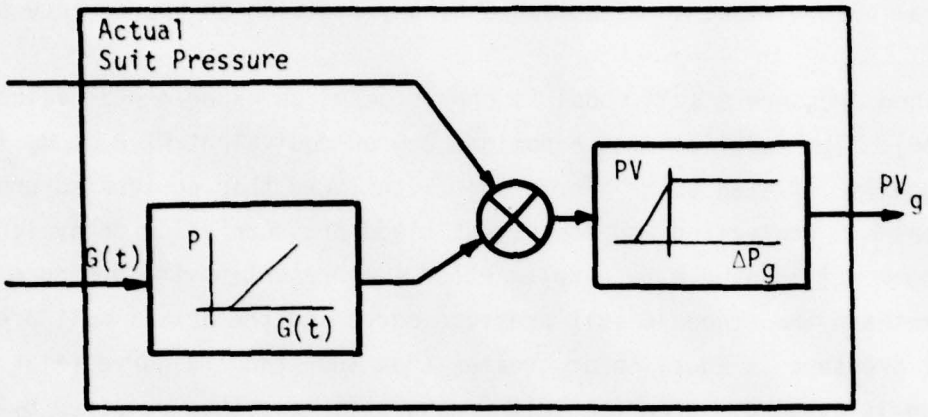

LEGEND

G(t)	=	Acceleration Vector in G_z axis
P	=	Scheduled Suit Pressure
PV	=	Intermediate protection value
ΔP_g	=	Difference between required and actual suit pressure
PV_g	=	Suit protection value

Figure 6. G Suit Model for Generation of Protection Value PV_G

The Visual Model

Background

The effect that acceleration has on the visual apparatus is observed in terms of tunnel vision, greyout, and blackout. During the periods of greyout there are also decreases in visual acuity and brightness contrast detection ability. Although there are multiple factors related to the anatomy, psychology and physiology of the human which are responsible for these changes in visual perception, the structure of the eye is a primary factor and provides the basis for a usable model.

The approximately spherical eyeball contains an optical system which transforms light through a variable focus lens and forms an image on a light sensitive layer on the inside rear surface (Figure 7). Detected light in electrical signals that pass through neural links to the brain where conscious recognition of the image takes place. The eye is supplied by the opthalmic artery which has two branches in the eye itself. One branch, the retinal artery, enters the eye within the optic nerve and provides the primary source of blood to the retinal layers. The other branch, the ciliary artery, supplies the outer layers of the eye and the cilinary processes. The central retinal artery enters the eye at the nasal side of the optic disc. Within the disc margin the artery divides into a superior and inferior branch and these branches then divide into temporal and nasal branches. These four divisions supply the four quadrants of the retina and can be observed in vivo by means of the opthalmascope. The branches are actually arterioles without precapillary sphincters (13).

The retina is composed of distinctly different areas, the optic disc which is the entry point of the neural links to the brain, the macula containing the foveal area which is the optical center of the eye, and the parafoveal areas. The principal light detection apparati of the eye are the rods and cones which are distributed throughout the eye with varying densities in the different areas. There are no rods or cones in the optic disc area and therefore the disc represents a blind spot on the retinal field. The fovea contains the greatest density of rods and cones and therefore provides the greatest visual resolution. The peripheral areas of the retina have a greater recruitment of sensors per neuron and thus have a lower resolution.

The neural linkages between retina and brain are also distributed with varying densities to the rods and cones. In the peripheral areas containing

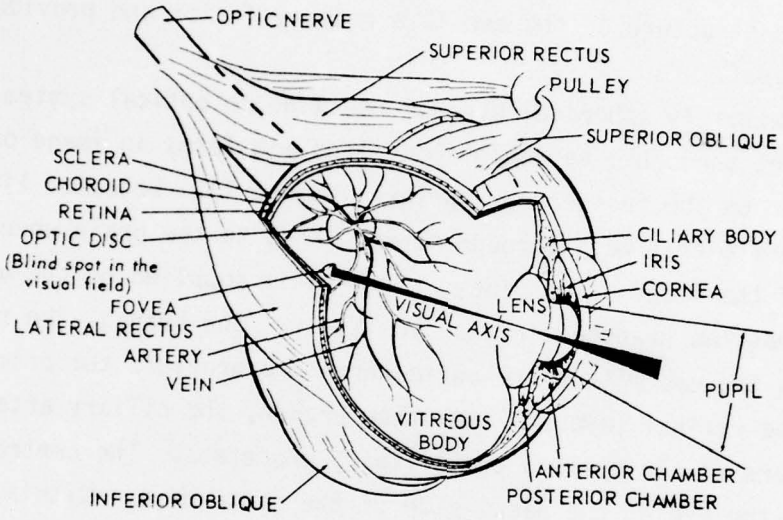

Figure 7. Topography of the Eyeball
from W.J. White in Reference 60

only rods, there is a recruitment or summation of detectors so that one neuron may serve multiple rods. In addition, the visual pathways have 3 cells and 2 synapses within the retina (see Figure 8). These neural junctions are particularly susceptible to oxygen deprivation and the peripheral blackout phenomena is thought to be at the ganglion level in the chain (37). The rods and cones in the fovea region are innervated on a nearly one to one basis.

The eye is maintained at an internal pressure which is above that of the surrounding tissue. This intraocular pressure ranges from 10 to 20 mm HG in the normal eye. This internal pressure serves to hold the eye relatively rigid thus supporting its optical apparatus. Any fluids which are transported into the eye must enter at some pressure greater than the intraocular pressure. When the blood pressure supply drops below some critical point the retinal supply vessels no longer remain open to blood flow. Therefore, theory predicts that visual field collapse in $+G_z$ acceleration occurs when retinal artery pressure approaches intraocular pressure and retinal perfusion ceases. In 1954, Lewis (40) examined the retina directly with a funduscope and drew illustrations of the retinal supply at $+G_z$ accelerations. In 1968, Newsome (48) using color photography confirmed that blackout is characterized by pallor of the optic disc and drainage of blood from the central retinal artery and vein. Thus it is evident that sufficient pressure in the opthalmic artery is necessary to insure delivery of nutrients and oxygen to the retinal layers.

The simulation model utilizes these concepts and offers a systematic look at the blood pressure distribution across the retinal field. The changing pressure levels which are postulated across the eye serve as a partial explanation and a functional model for the prediction of field changes other than total blackout. The model requires an oversimplification of detailed circulation patterns and draws upon certain observations in the literature on the anatomic structure of the eye.

The Visual Field Model

The structure at the retina is idealized as a network of cylindrical hydraulic pipes with a central supply at the entrance of the optic nerve, Figure 9. If a steady laminar flow is assumed through a cylindrical tube the flow (Q) will vary with the 4th power of the radius of the tube and the pressure differential ΔP. Also the flow will vary inversely as the length ℓ of the tube and viscosity of the fluid η. This is stated in Poiseuille's law as:

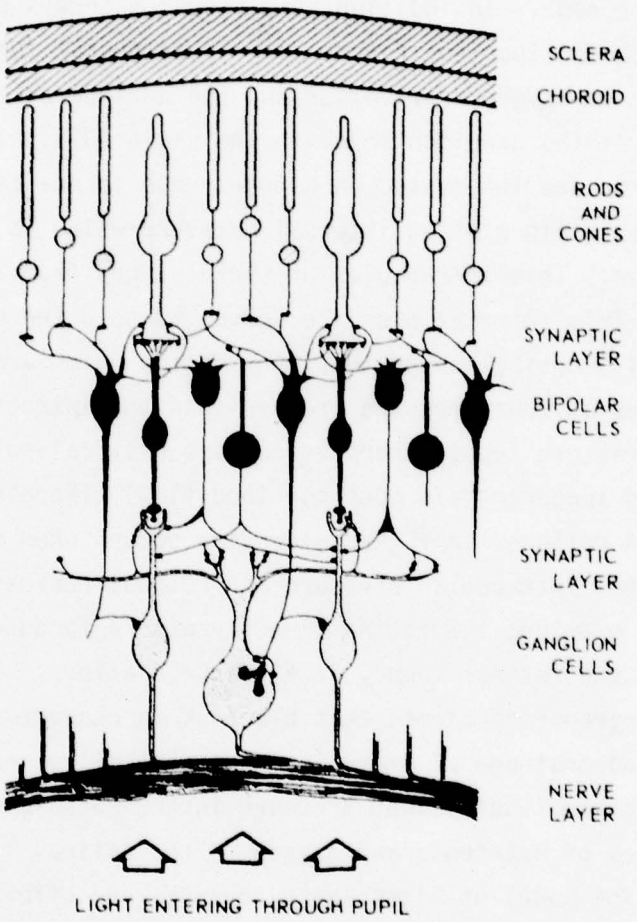

A schematic diagram of the retina is shown in cross section, with the forward facing surface below on the drawing and the rearward layers above. Notice that light from the lens falls first on the nerve fibers, traversing these and two layers of ganglion cells before reaching the primary light sensitive cells, the rods and cones. There are many more rods than cones, but in one small area of the retina there are cones only. This rodless area is the fovea, the area of sharpest day vision. Cones are responsible for vision at the higher illumination levels, and for color vision. The rods are able to handle the lower light intensities of twilight and night. Nerve pathways from the different cells cross and interconnect at the ganglion layers, as illustrated.

Figure 8 Schematic Section of Retina from White. (57)

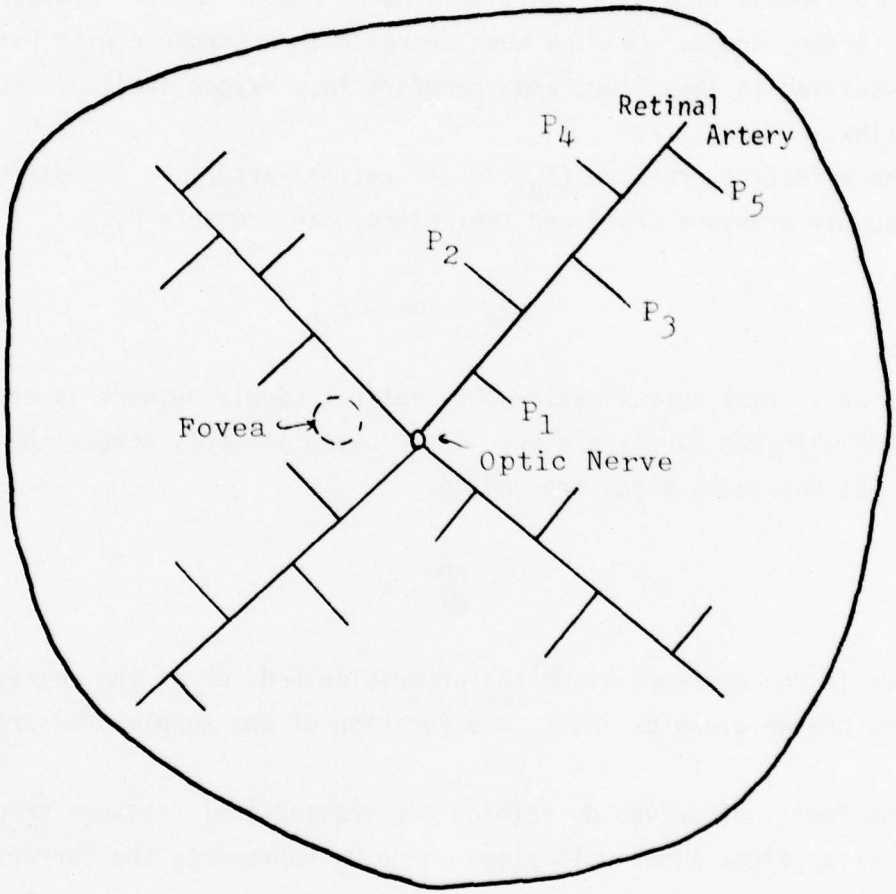

LEGEND

$P_1, P_2 \ldots$ = Pressure in mm Hg at various distances from Optic disc. $P_1 > P_2 > P_3$..etc.

Figure 9. Linearized Representation of Blood Supply to the Retina

$$Q = \frac{\pi r^4 (\Delta P)}{8\eta \ell} \tag{12}$$

The blood pressure drop across the cardiovascular system is mostly across the arterioles (2). At higher levels of pressure the retinal arteries supply the arterioles with sufficient pressure so that the entire retina is perfused with a continuous flow of freshly oxygenated blood. As the pressure in the retinal artery drops, the flow must decrease in accordance with Poiseuille's Law, resulting in less blood and therefore less oxygen available to replenish the retina.

The effective pressure (P_R) in the retinal artery is the difference between supply pressure (Pae) and the interocular pressure P_{IO}.

$$P_R = Pae - P_{IO} \tag{13}$$

As an initial approximation, the retinal supply network is assumed to be a network with the supply pressure distributed linearly across the network. That is at any point along the supply:

$$\frac{dP}{dx} = K_i$$

where dx is the distance along the arteriolar bed, dP is the corresponding pressure change along dx and K is a function of the supply pressure at the optic disc.

The family of curves describing the transretinal pressure gradient is a series of straight lines with slope where P_R represents the current retinal

$$-\frac{P_R}{K_4}$$

pressure at the disc and K_4 is the outer circulation limit of the retina, coresponding with the ora seratta. For any value of Pae the retinal pressure as a function of distance from the disc is given by:

$$P_r = -\frac{P_R}{K_4} x + P_R \tag{14}$$

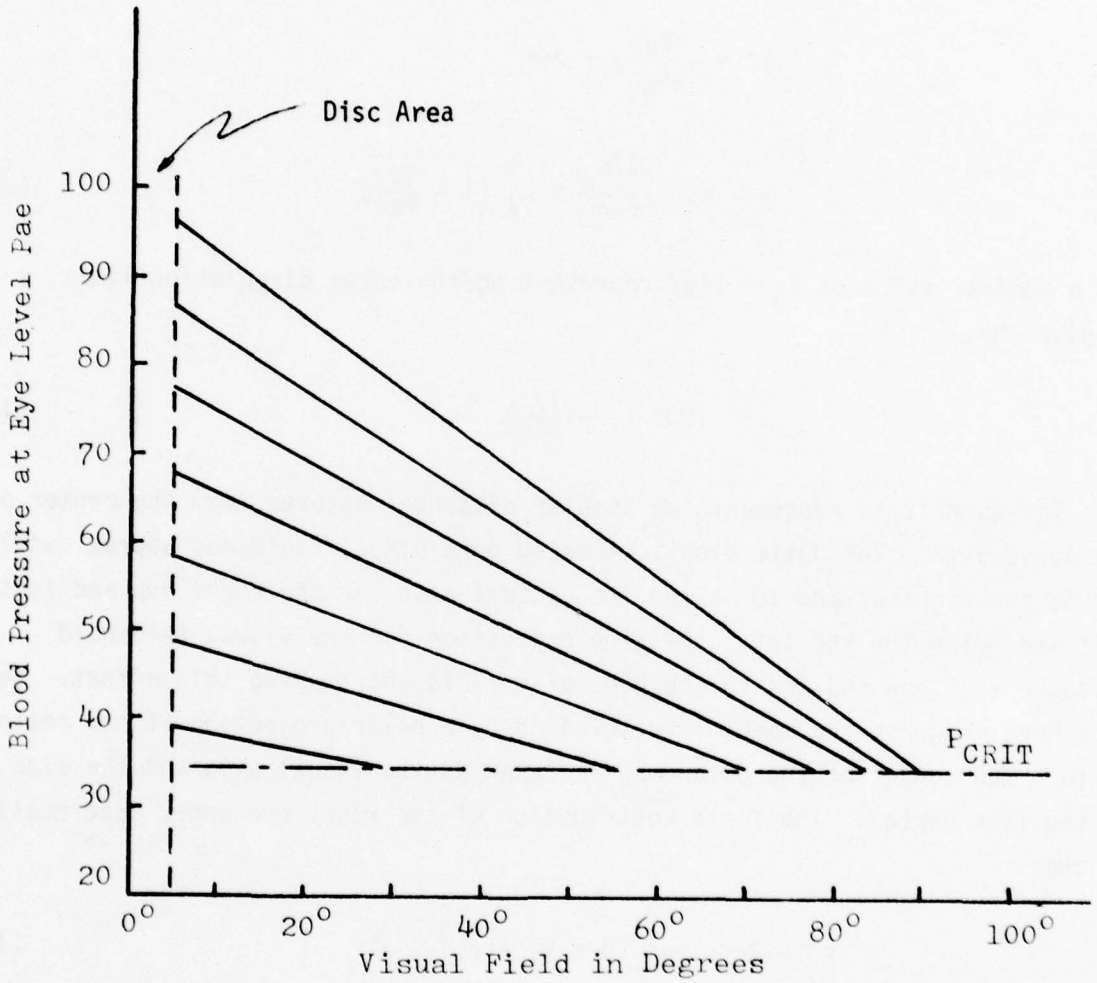

LEGEND

Pae = Arterial Pressure at eye level

P_{CRIT} = Pressure required to enable flow in arteriole

Figure 10. Poiseuille's Law Applied to the Retina where $dP/dx = K_i$ for Various Pae

In a small blood vessel a pressure differential of about 15-20 mm Hg across the vessel wall is required to maintain an open flow channel (2). When this transmural pressure is not maintained, flow will cease and the blood supply is cut off to all points beyond. This critical pressure is now labeled P_{CRIT}.

$$17 = -\frac{Pae}{K_4}x + Pae$$

$$x = K_4 - \frac{17K_4}{Pae} = K_4\left(1 - \frac{17}{Pae}\right) \tag{15}$$

For a nominal value of $K_4 = 110°$ representing the outer circulation limit, x is given by:

$$x = 100°\left(1 - \frac{17}{Pae}\right) \tag{16}$$

The quantity x represents an angular distance measured from the center of the optic disk. The optic disk is located on a visual field map approximately 10° to the right of and 10° below the optical axis for the right eye and to the left and below for the left eye. The expression for the visual threshold distance x is now applied to the binocular field chart using this offset. The peripheral edge of the model is determined by a polar projection of the retinal field. The center of the polar map is taken as the visual axis and the disc as the flow center. The field contribution of the right eye under acceleration is then:

$$r^2 - 2r_d r \cos(d + x) + r_d^2 - x^2 \tag{17}$$

where r is sensed visual limit at χ, r_d is offset distance of the disc from the visual axis and d is the angular offset of the disc from the horizontal axis. A similar expression is found for the left eye.

The visual field model can now be extended to a binocular field. Figure 11 is a binocular field map showing the coincidental foveal areas as the visual center, and the optic disc for each eye in a manner that depicts the observed field from inside out. The outer lines depict the outer edges of the peripheral vision. Lowered blood pressure supply in each of the modeled retinas causes the

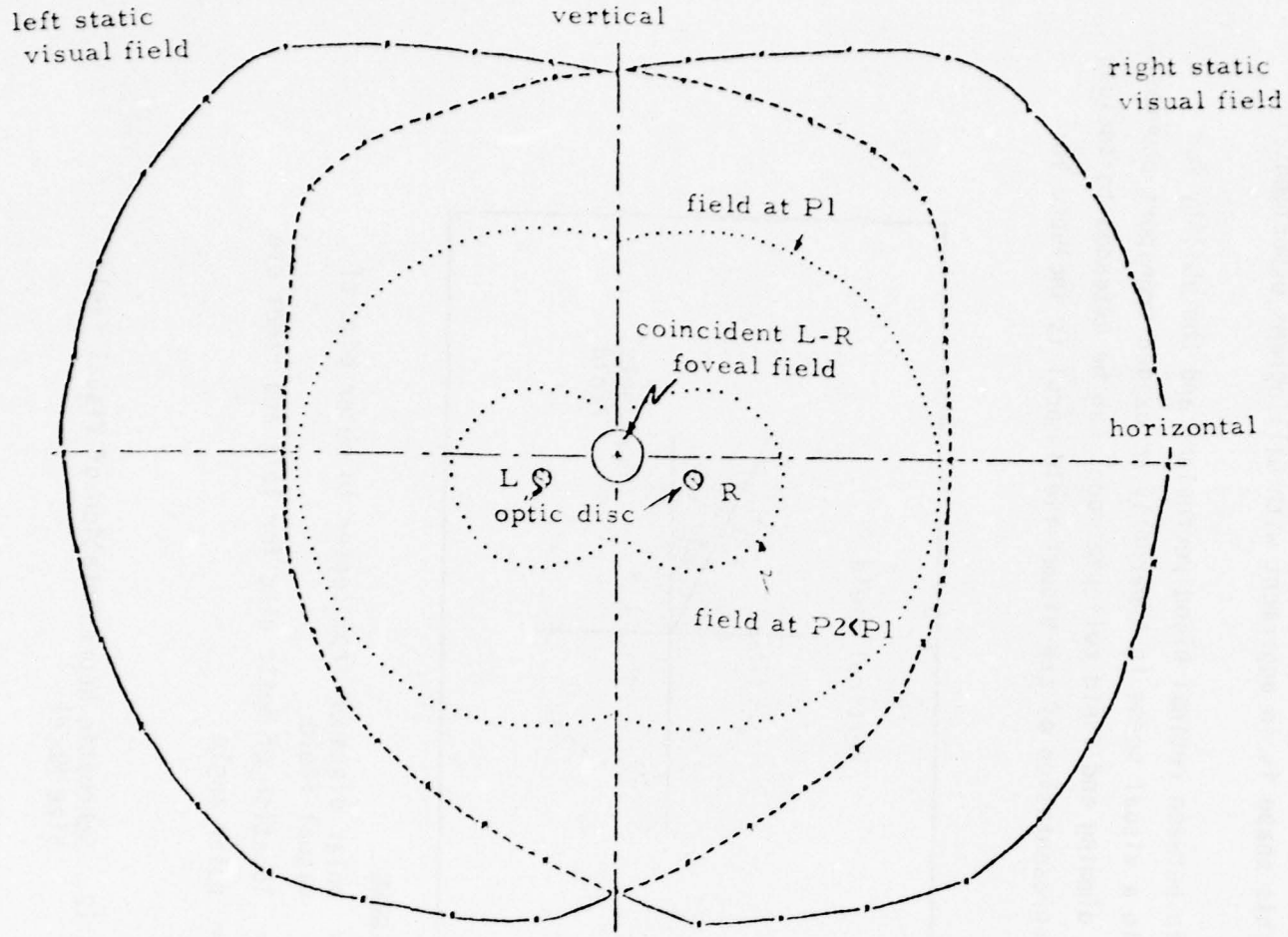

LEGEND

P1,P2 = Arterial Pressure at the Disc.

Figure 11. Binocular Visual Field Decay Due to Reduced Blood Supply Pressure

field to collapse as concentric circles with centers at each of the optic discs as shown by the dashed lines. Thus the visual field collapses toward a somewhat oval shape with the vertical field having a smaller visual angle than the horizontal field. This shape is in aggrement with Gillinghams experimental results (18).

The relationship between retinal blood perfusion, and the ability for contrast detection in a visual scene is apparently an oxygen transport phenomena. The observed visual dimming and field collapse model can be extended to include these effects. A representation of the visual field model is included in Figure 12.

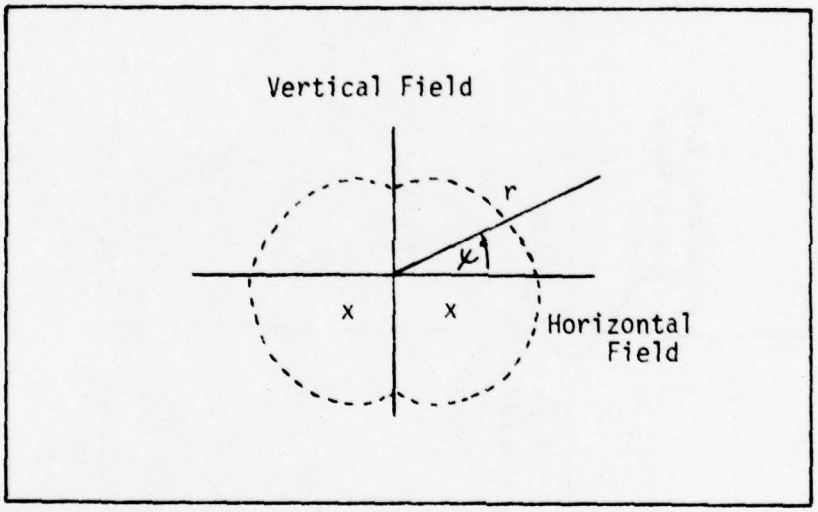

LEGEND

r = polar distance from center to outer edge of visual field

x = location of optic disc for left and right eye

φ = polar angle

Figure 12. Schematic Representation of Visual Field Size Model

The Straining Model

Background

Human tolerance to acceleration may be improved by the use of protective measures and devices. Straining and grunting in tight turns was practiced by

German pilots prior to World War II to improve their tolerance. This technique gradually evolved into the M-1 maneuver. At the same time it was discovered that bending forward also improved the tolerance of pilots in high acceleration maneuvers. The effects of posture, restraint, and body position on G tolerance have been well worked out and have been reviewed in detail (15, 16).

The M-1 maneuver, defined as muscular straining with expiration against a partially closed glottis, (see Appendix A) is a most effective voluntary protection against the circulatory effects of $+G_z$ acceleration (43, 58). The physiologic basis for this protection has been ascribed to its effect on increasing the arterial pressure during acceleration. As forced expiration is instituted, the resulting increase in intrathoracic pressure is transmitted directly to the aorta. There is an immediate increase in peripheral arterial pressure which is only slightly less than the increase in intrathoracic pressure. This maneuver affords up to 2.4 G protection against blackout (5). The circulatory mechanisms described were identified by Rushmer in 1946 (49). The "pressure raising" approach has theoretical difficulties in that blood pressure is controlled within rather narrow limits by a number of effective servomechanisms, the baroreceptor system being the best known. The elevated intrathoracic pressure can result in a decreased venous return, lowered cardiac output and therefore a lower blood pressure at the eye. The carotid sinus reacts to the initially increased blood pressure and also to attempt to regulate the blood pressure. Both of these effects are minimized by a cyclic application of the M-1 or I-1 procedure with a repetition rate of 4-5 seconds (Appendix A).

The vestibular-cerebellar system senses the initial G force and in fact may anticipate it in the real sense as the cerebeller function has multiple inputs to key it to oncoming acceleration. For example in the aircraft it is an initial cerebral activity that initiates the maneuver and therefore the system has apriori knowledge of the magnitude, onset rate and duration of the upcoming acceleration profile. The centrifuge subject has some keying from auditory senses originating from hydraulic valves, start up commands as well as early motion cues to predict that something is going to happen. The simulator pilot has cues in that his actions generate the profile. Of course in a well designed test, the subject may not have apriori information on the G profile.

The action of the vestibular-cerebellar system modifies the neurologic system in a manner which leads to increased anticipation and undoubtedly higher

sympathetic activity, i.e. increase muscle tone. The anticipatory activity involving such anxiety then changes the hydraulic constants of the cardiovascular system. This of course affects the peripheral resistance, damping and blood pooling capability and the natural frequency of the P-G transfer function.

Investigations by Lind and his coworkers on the effects of isometric exercise have also identified cardiovascular responses to sustained muscular contraction (41, 42). For example, a 50% maximum voluntary handgrip contraction can raise mean arterial blood pressure 66 mm Hg. The mechanism of the response has not yet been established. The tensing or isometric exercise of skeletal muscle has been mentioned as a G protective factor (36, 43) but no attention has been given to the cardiovascular mechanisms involved. Muscular tensing has been alleged to decrease the amount of blood pooled in the legs and abdomen and to increase peripheral arterial resistance. Muscle tensing alone has been reported to elevate blackout threshold by about 1G although the muscle groups used and the force exerted were not specified (37).

Use of the M-1 and L-1 maneuvers to increase the eye-level blood pressure, and therefore the acceleration tolerance, carries with it an implicit use of energy stored within the body. There is therefore, a energy cost to a pilot undergoing acceleration stress in maintaining this visual function through increased blood pressure. When the subject is close to the relaxed acceleration tolerance limit, straining is required to increase that tolerance level. The increase being essentially equal to the amount of elevated blood pressure that can be generated with the straining. The energy expenditure is apparent in the protective maneuvers used. The closer the subject is to a limit, the greater the required straining. The acceleration force also reduces his ventilation rate and reduces his pulmonary efficiency. This further compounds the problem of maintaining appropriate oxygen as well as blood pressure in the eye and cortial tissues. Thus, there are "at least" two important components contributing to the reduction of energy reserves. These are the closeness to the cardio-vascular limit and pulomonary efficiency. Once the pilot has exceeded the normal G-stress level, represented relaxed tolerance, even more energy must be expended to increase the blood pressure and thus maintain vision.

The rate at which energy is expended in the blood pressure maintenance task is a factor of the straining efficiency, G-suit efficiency, and the magnitude of the G-difference between his relaxed tolerance and the current G-stress level. His energy expenditure may be a factor in determing the time

endurance limit within the acceleration profile. The pilot is working in an essentially oxygen deprived situation because of the blood-lung field shifts which may not allow for continued replenishment of the oxygen within the blood. This exercise activity of the pilot involves both aerobic and anerobic activity. The aerobic portion of energy production utilizes glycogen and free fatty acids as well as oxygen. The aerobic oxidation of a molecule of glucose yields 38 molecules of ATP. Contrast this with the 2 molecules of ATP produced in the anerobic metabolism of glucose to lactic acid. It is obvious that the pilot, to endure the acceleration profile for the longest time, should be performing an aerobic exercise. However, the limited pool of oxygen that is available and the activity of straining suggests that the activity in exercise in the L-1 and M-1 maneuver is both aerobic and anerobic. The anerobic activity can only be continued for the period of time that ATP is available. The act of straining reduces blood flow in the active muscle and exacerbates the oxgenation problem. The exercise intensity may then determine the metabolic pathway utilized in performing the M-1 and L-1. If the greater amount of exercise performed in straining for acceleration tolerance improvement is essentially anerobic, then it would seem that an anerobic training method would be most beneficial for pilots rather than an aerobic training method. The protection factor generated by the breathing pattern is critically controlled by the straining and breathing rate. An improperly performed M-1 can actually reduce protection and result in a detrimental pressure drop.

The response of blood pressure to the valsalva maneuver is depicted in Figure 13. From a nominal value of 125 mm of mercury at the onset of the L-1 maneuver, the blood pressure is increased to a value of 160 mm Hg by use of the L-1 or valsalva maneuver. As the technique is continued, the blood pressure gradually decays back to normal or the 125 mm Hg value. It can be surmized that the L-1 or valsalva is important in raising blood pressure if that maneuver is maintained for a short period of time (between 3 and 5 seconds) and then repeated at some short interval after that to maintain the higher level blood pressure. The reason for the falling blood pressure after the extended period of valsalva maneuver is that the blood return to the thoracic cavity is inhibited by the higher pressure generated by the maneuver. With less blood available, the heart is unable to effectively maintain a suitable pressure output.

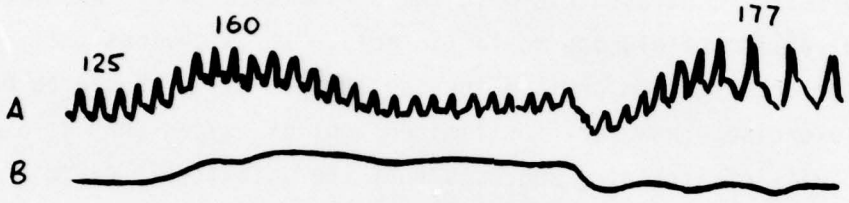

LEGEND

A. Arterial Pressures in mm Hg.

B. Intrathoracic pressure

Adapted from Hamilton et al. (26)

Figure 13. Valsalva Maneuver

In the recovery period, that is after the valsalva maneuver has stopped, there is also an overshoot period wherein blood, now rushing back to fill the heart, is expelled with greater force and the blood pressure increases after the valsalva maneuver. This may well be a secondary effect which can be useful in determining both repetition rate and time period of application of the L-1 or valsalva maneuver. Thus this CV response provides clues as to modifications of the M-1 maneuver and its applications.

A similar effect is seen with acceleration induced blood volume shifts. If a quantity of blood is returned to the stressed heart by a positional change there is a brief period of elevated pressure (31). The transient pressure rise may be an important consideration in sequencing acceleration protection devices.

Model Implementation

Figure 14 represents a descriptive model used to implement the known responses and repetition rates of the M-1 maneuver. The M-1 maneuver, or modified valsalva maneuver is most efficient at intervals of 3-5 seconds. Periods of straining for the maneuver which are less than 3 seconds are not as effective at reaching the maximum blood pressure. Periods of straining which extend beyond the 5-6 second time period involve the blood return to the heart problem and therefore are also less effective at maintaining the higher blood pressure. The actual blood pressure achieved by a given straining regime is difficult to determine. In fact the blood pressure achieved is essentially a function of the pilot's control strategy in maintaining his function within the acceleration profile. Figure 15 represents the straining protection model based on the physiology and the past research information. On the input side of the model, the letter E represents a control strategy or the amount and duration of straining which is a function of the pilot's training. The model is characterized by a gain value related to the straining level. The dynamic terms reflect the activity of the muscle and neural systems and the changes in the blood flow.

Further research is needed in elucidating the effects of the L-1 and M-1 in terms of frequency response characteristics, overshoot times and other important factors related to a control model.

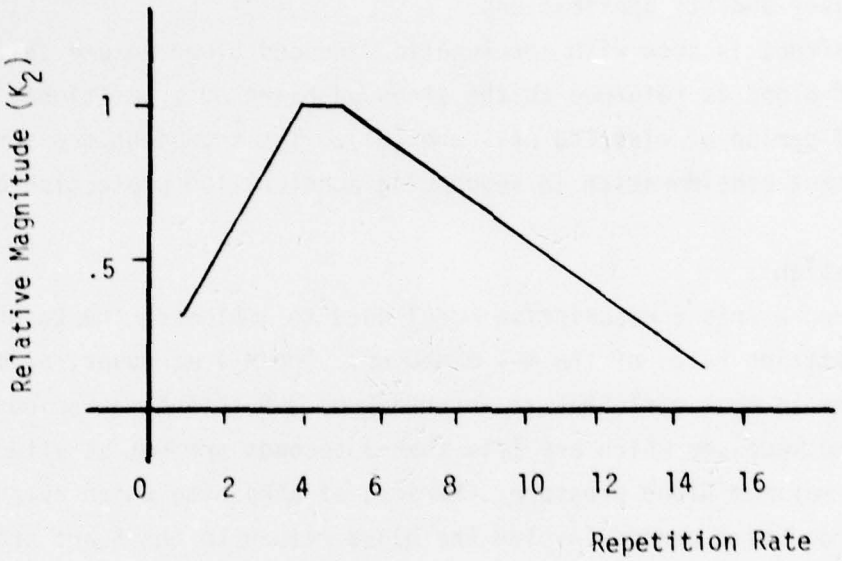

Figure 14. Effect of Repetition Rate on Straining Protection Value

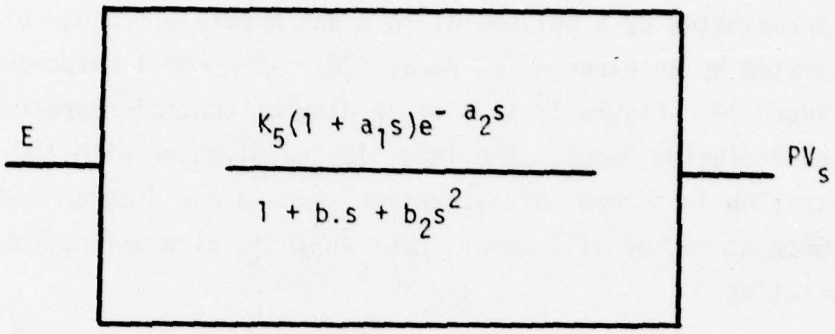

LEGEND

E	= Effort Strategy
K_5	= Gain for Straining Protection Value
$a_1, b_1 ..$	= Time constants
s	= Complex frequency
PV_s	= Straining Protection Value

Figure 15. Straining Protection Model

The Ventilation Perfusion Model

Background

Distortion of the lung field during acceleration causes serious changes in the ability of oxygen to be transported across the lung surface and thence into the blood. A number of methods have been used to describe the oxygen transport across the lung. Glaister has summarized a number of these in his book (21). The causes for the change in oxygen transport appear to be due to blood shunts caused by the redistribution of the blood field across the lung at the lower levels and due to the absence of blood at the upper levels of the lung. To establish a linear model of such a system is an extremely difficult problem. One method of attack has been proposed by Holden and Rogers and is used as a basis for the model development in this system (28). The overriding concern is that one develop a dynamic model which shows the oxygen concentration changes as a factor of acceleration stress. If the model output matches the known information, then the input assumptions are at least realistic and the basic research principle is then established to allow for further study.

Model Development

A summary of the model development shows that the arterial oxygen concentration can be approximated by a polynomial in G and a rate of change of the oxygen can be approximated by an exponential decay (28). The model response to G-force is shown in Figure 16. Figure 17 is a block diagram control representation of the Ventilation-Profusion Model. The input is the G-vector with the output the oxygen concentration in percent of saturation. The block diagram model clearly shows the polynomial factor of G as an input which is also a function of the G-vector orientation.

The Energy Stores/Oxygen Model

Background

The energy production capability of the human is related to proportions of fats, carbohydrates and proteins used as metabolic fuel and is related to the amount of oxygen available to use these fuels in the production of energy. The actual energy stores of the body in terms of how much work the human is capable of is difficult to measure. The human, like all physical systems, however, is constrained by basic laws of thermodynamics. We can, therefore, make the simple assumption that a model can be developed which is related to oxygen intake and energy output. Although this model might not be accurate in a micro-sense, certainly it should hold true over a long period in a macro-sense.

The energy stores model, then, is an energy balance system in which oxygen is proficed through the pulmonary system. The oxygen is utilized with the metabolic fuels in the straining system with the resultant higher blood pressure through the straining. Other oxygen is utilized in normal metabolic maintenance and the oxygen reserves are depleted. If all factors are related to equivalent oxygen levels, and assumptions are made on the percentage of aerobic and anerobic activity, then the energy balance equation is written as:

> Oxygen reserves + oxygen intake = oxygen expended in straining activity + oxygen expended in normal basic metabolism

or more precisely:

$$\sum_{n=1}^{m} \int_{o}^{T} E_n O_2 dt = C_1 \qquad (19)$$

where $E_n O_2$ represents the oxygen dependent system n and C_1 is a constant.

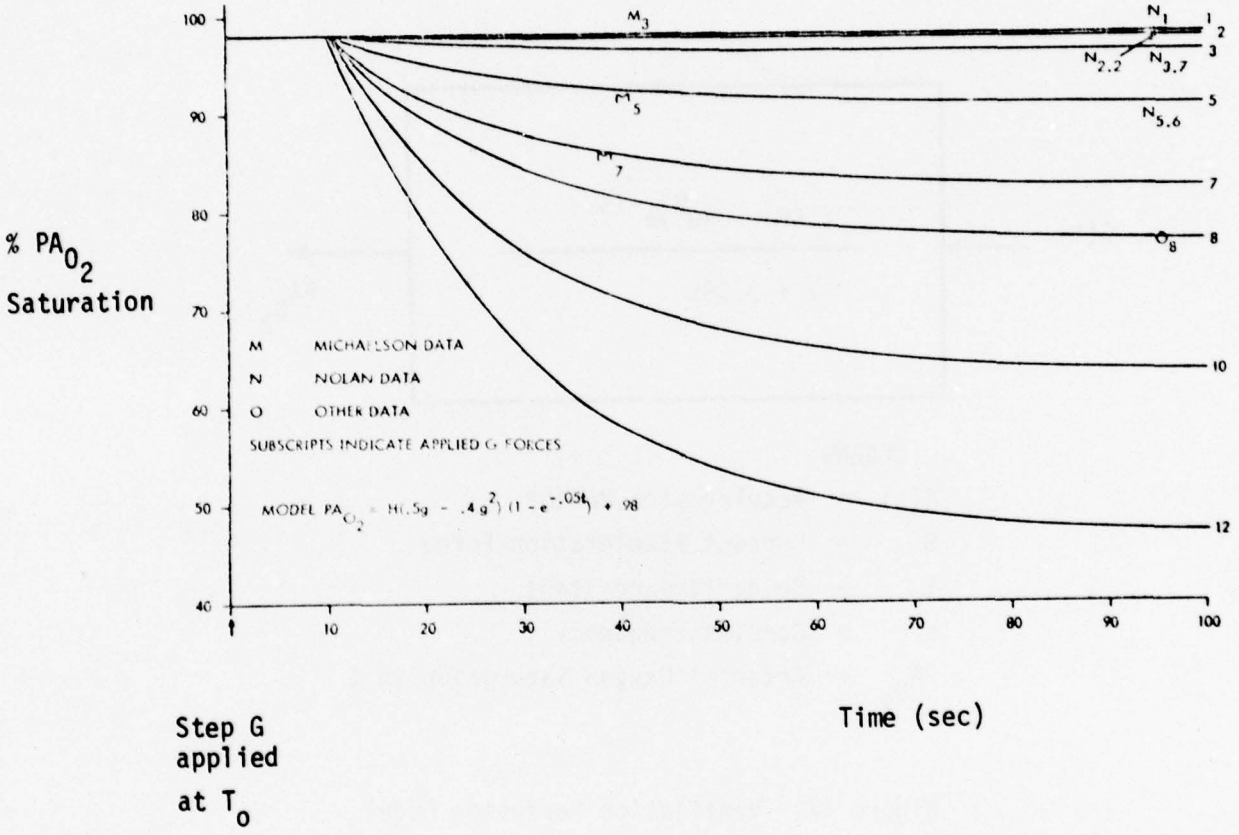

Figure 16. Ventilation Perfusion Model Response to Step G force. From Holden, Rogers. (28).

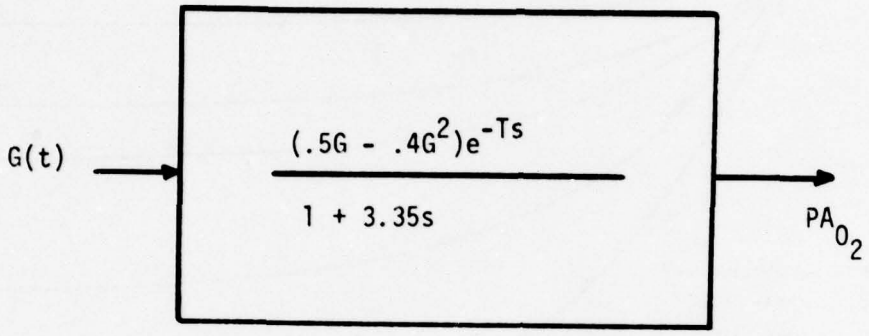

LEGEND

G(t) = Acceleration Vector

G = Current Acceleration Force

T = Delay time constant

s = Complex Frequency

PA_{O_2} = Arterial Oxygen Saturation in %

Figure 17. Ventilation Perfusion Model

Model Development

The energy system is modelled as depicted in figure 18. The straining protection model driven by the effort strategy that the subject or pilot has adopted to provide protection, provides a value to the system which is related to elevated blood pressure. This value is PV_S, protection variable from straining. The effort strategy that the subject or pilot has adopted also causes energy expenditure. This energy expenditure depletes the energy stores represented by the small block indicating the percent of oxygen saturation normally found. The Ventilation Profusion Model at the bottom of the figure, with an input of acceleration as a function of time, adds to the energy stores and increases those stores in a fashion dictated by the control model formulation of the Ventilation Profusion block. The output of the model is, the level of oxygen in the blood and a protection value which provides the input to other sections of the model. The Energy Expenditure Model is simply an integrator which integrates the energy effort and translates this to a depletion of the oxygen stores in terms of a decreased percent of oxygen.

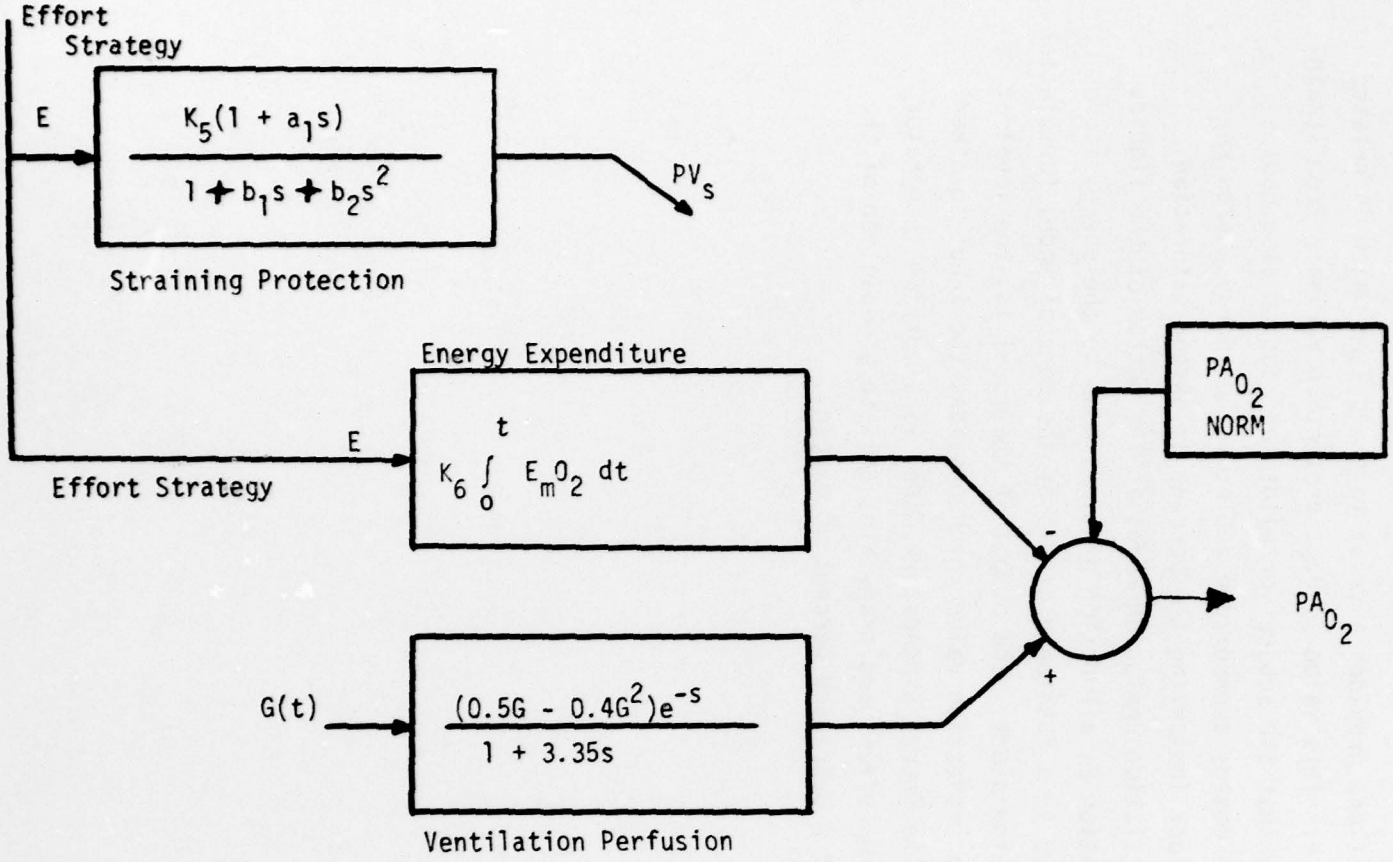

LEGEND

K_5	=	Straining Protection Gain	G(t)	=	Acceleration Vector
PV_s	=	Straining Protection Valve	G	=	Current Acceleration level
E	=	Effort Strategy	PA_{O_2}	=	Arterial Oxygen Saturation %
$a_1, b_1 ..$	=	Time constants	K_6	=	Conversion Factor to PA_{O_2}
s	=	Complex frequency			
E_m	=	Oxygen Consuming System			

Figure 18. Energetic System Model

SECTION 3

SYSTEM INTEGRATION

The Simulation Model

The Simulation Model representing the concept of an energetic system applied to acceleration stress is brought together in Figure 19. When the pilot or subject is exposed to an acceleration profile indicated by $G_{(t)}$ the cardiovascular system responds with a decreased blood pressure at the eye if the G has a component in the z direction. This response is represented as the Cardiovascular Model. The G suit is modelled as a system which responds to the acceleration vector and increases the protection value (blood pressure). The acceleration signal affects the Ventilation Perfusion System Model by decreasing the inflow of oxygen to the available energy pool. The reduced protection value (blood pressure) and the reduced PAO_2 value reduced (oxygenation of the blood) affect the Visual System Model by changing the visual information channel. The visual changes are measured as alterations in the visual modulation transfer function (MTF). The Decision Model is affected by the visual changes MTF reduced protection value and PAO_2 value. A protection effort strategy is generated by the Decision Model and the Straining Models are activated. The Straining Models increase the protection value and decrease the available energy pool.

Thus the Energetics Model becomes one in which energy becomes a primary constraint and a concomittent result of the straining and acceleration profile. This concept ties the acceleration protection and the cost of the protection together in a single model.

The Optimal Strategy Model

A reorganization of the System Model and the addition of flight requirements now facilitates the application of an optimal energy and visual function control scheme. Figure 20 presents the required organization. The physiologic functions of pressure delivery are categorically identified under the pressure system block. The Energy System is organized from the Straining and Ventilation system. The Visual System is depicted as a function of pressure and oxygen supply. All three of the functions are input to a decision/strategy filter which evaluates the states of the functions, combines these with other functions

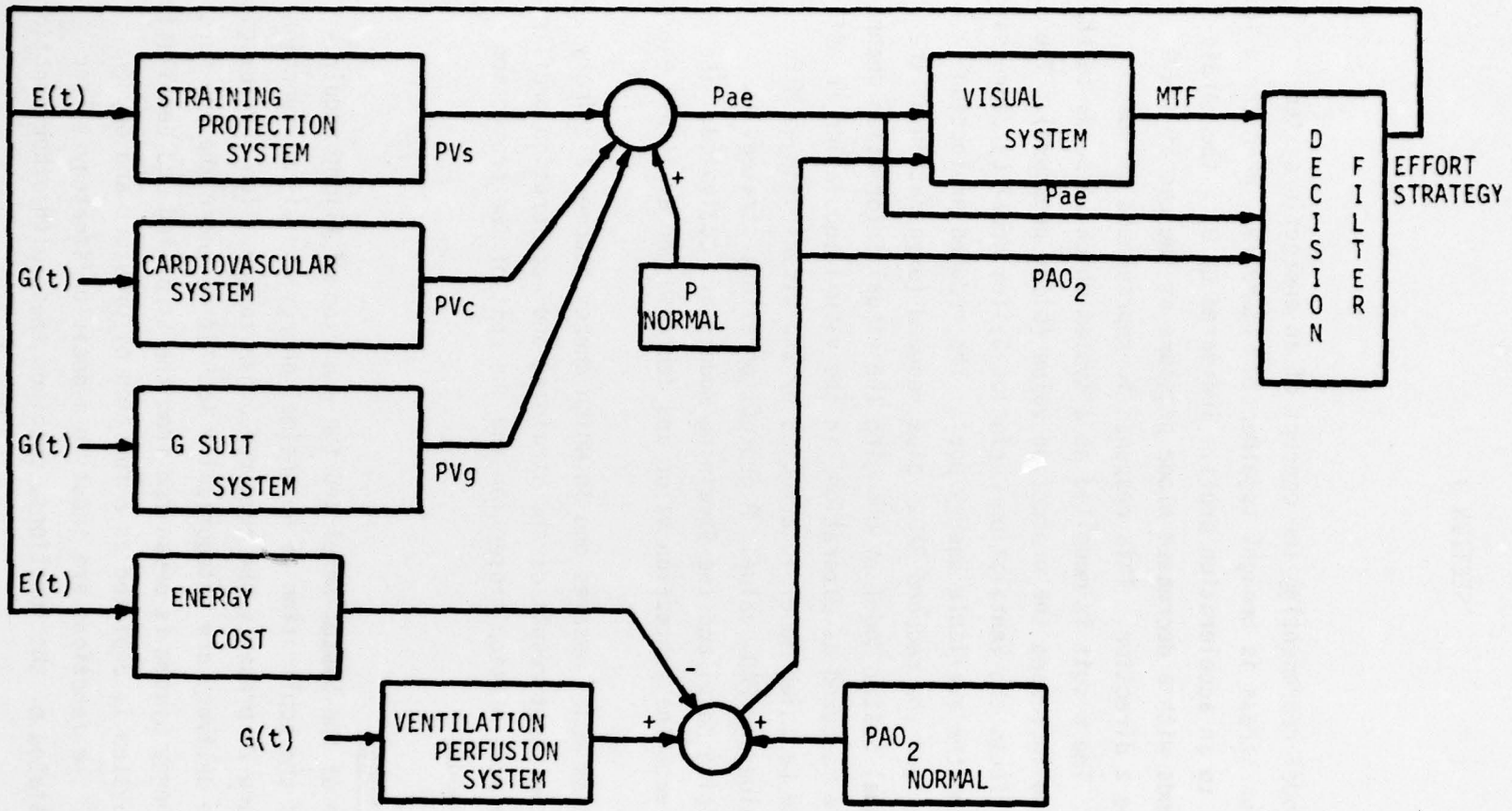

LEGEND

E(t)	=	Effort Strategy	PVc	=	Cardiovascular Protection Value
G(t)	=	Acceleration Vector	Pae	=	Arterial Pressure at Eye Level
PVs	=	Straining Protection Value	PAO_2	=	Arterial Oxygen Saturation %
PVg	=	G Suit Protection Value	MTF	=	Modulation Transfer Function

Figure 19. Integrated System Model

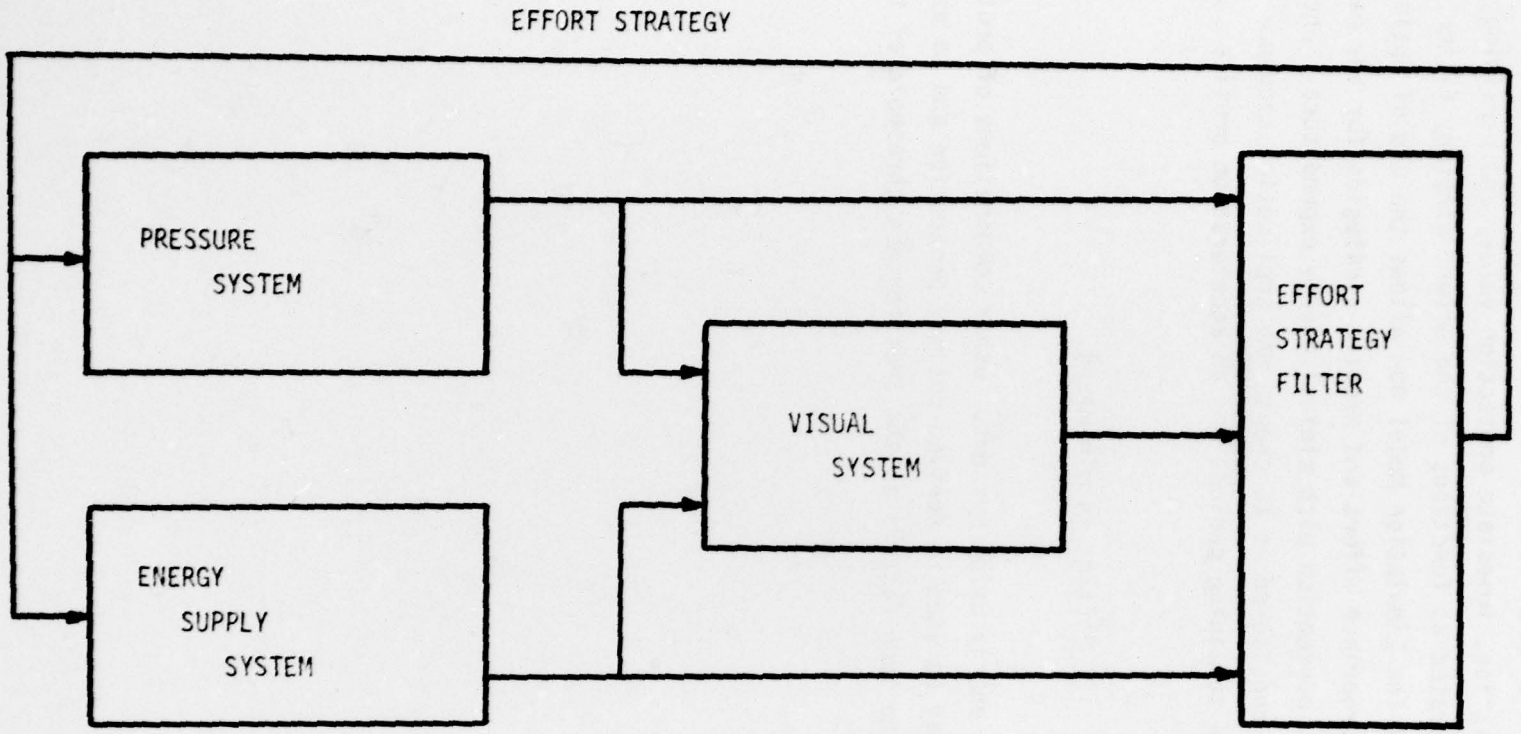

Figure 20. Effort Strategy Model

and generates an "effort" or protection strategy. In the Simulation Model the values of energy conservation, immediate protection value, and straining repetition rate must be generated as functions of the effort strategy filter.

The organization of the Simulation Model now allows the use of optimization techniques to define appropriate effort and profile strategies for the maximization of acceleration protection with minimal energy expenditure. One control law which might be considered is to choose the application sequence of protection equipment and straining periods for an acceleration profile such that

$$\int_0^\infty (E_n)^2(t)dt \text{ is minimized.}$$

where E_n represents the energy using systems. Other combinations of protection value and energy cost may be used to derived optimal protection and to establish the linking correlates to such factors as the indifference threshold of the Optimal Control Model.

SECTION 4

CONCLUSIONS AND RECOMMENDATIONS

The development of this model and submodels has been based largely on the experimental data available in the literature. The concept of energy as a portion of the model is defined in a very general sense. Using the available oxygen as an indicator of the energy is only the first approximation to a useful system model. This development leads to a new set of research directions which can be profitably followed for redefining acceleration physiology and performance models. The sub-models of this system are in no way the final models, but are only approximations based on information that was available at the time of this study. Each of the sub-models needs further exploration and further definition using a modelling technique which allows for integration with the larger model.

The difficulties, of course, are in the assumptions that each of the sub-models is a linear system and does not have a cross-coupling affect with the other sub-systems. These linkages and couplings can only be studied after more refined models have been developed. In fact, further research may redefine the structural model as laid out here and in doing so hopefully will bring us closer to the point wherein it can be used as an optimal protection model. The decision model will provide links with the optimal performance models used in performance evaluation.

Optimized Protection System Sequencing

Evaluation of the model dynamics in an optimal control strategy system provides a new look at the concepts of acceleration tolerance. Using optimization techniques it is possible to define performance/protection stragegies for specific combat maneuvers. A strategy or a maneuver can be tailored to extend either the period of sustained acceleration tolerance or extend the level of acceleration tolerance. A balance between the tolerance level and period can be adjusted with the simulation algorithm.

Protection strategies can be developed which relate to increased protection values based on the dynamic responses of the human, the dynamic responses of the optimal strategy. It is not unreasonable to expect that acceleration protection methods can be improved by evaluating the model using Optimal Control Strategies.

The resulting protection sequence strategies will require advanced development of protection equipment. The new equipment philosophy must be based on the requirements of the maneuver dynamics as well as current acceleration level. Among these requirements are, varied seat tilt times and angles under acceleration, G suit pressure and fill schedule timing including couterpulsation, and more energy effective use of the straining maneuver. It is a realistic consideration that such sophisticated procedures will require the use of computational equipment which both monitors the human and is monitored by the human.

Straining Energy Cost

The dynamics which relate the straining maneuver to the increase in eye level blood pressure are an important question yet unanswered. There is little or no experimental evidence which allows an accurate description of the dynamic increase in blood pressure as a function of straining under acceleration. The time delays between straining onset, EMG output, and pressure elevation may be significant and may lead to acceptable but unwanted inaccuracies in the straining model. The delay time between straining and appearance of the EMG potential is on the order of 200 ms and is not significant in terms of the response times of the cardiovascular system. Quantification of the actual straining energy cost which is done in a particular protection maneuver can be done using the EMG signals of the major muscle systems used in developing the straining maneuver. The EMG straining information should be accompanied with information of intrathoracic pressure used to generate the higher blood pressure at the eye, and oxygen costs for the maneuver. A comparison of these values should be used to update and refine the model which expresses the energy-to-blood pressure protection level value.

Performance and Workload

The model provides an alternate structure to link acceleration physiology and performance systems. The combined effects of the reduced perfusion pressure and the reduced oxygen saturation at the cortex provides a secondary basis to re-evaluate performance which has been studied only in terms of oxygen deprivation. Studies which better define oxygen transport across cell structures at reduced pressure levels are an important requirement. The subset of models which describe the energy balance concepts and the effort strategy have a identifyable relationship with the Optimal Control Model (OCM) indifference

threshold. This subset also is an important consideration in work load measurement. In addition the physiologic basis for the retinal modulation transfer function provides a direct input to the OCM parameter for observation noise.

Visual Transfer Function

The blood perfusion schema of the retinal structure with some experimental validation could lead to predictive methods for describing the retinal-eye modulation transfer function. Thus, the modulation transfer function becomes a rational input to some Optimal Strategy Model in which the pilot is able to balance impaired vision and the required energy expenditure, to maintain an optimal visual function for a given mission situation. A promising extension of the visual model would include a dynamic representation of oxygen transport at the synapse junctions in accordance with Miller and Green (45). Reduction of oxygen concentration levels due to impaired pulmonary function or exercise would play an important role in this extended model. The distribution of visual receptors and their activation levels may yield a physiologic basis for predicting changes in the modulation transfer function of the eye during acceleration.

APPENDIX A

THE M-1 AND L-1 STRAINING MANEUVERS (20)

M-1 Maneuver

"Pilots commonly refer to the M-1 Maneuver as the "grunt" maneuver since it approximates the physical effort required to lift a heavy weight. The M-1 maneuver consists of pulling the head down between the shoulders, slowly and forcefully exhaling through a partially closed glottis, and simultaneously tensing all skeletal muscles. Pulling the head downward gives some dgreee of postural protection (shortens the vertical head-heart distance): inthrathoracic pressure is increased by strong muscular expiratory efforts against a partially closed glottis; and the contraction of abdominal and peripheral muscles raises the diaphragm and externally compresses capacitance vessels. For long-duration G exposures, the maneuver must be repeated every 4 or 5 seconds. When properly executed, the exhalation phase of the M-1 results in an intrathoracic pressure of 50 to 100 mm Hg which raises the arterial blood pressure at head level and thereby increases +G tolerance at least 1.5 G. *The inspiratory phase of the* M-1 maneuver must (be done as rapidly as possible, sic.)."

L-1 Maneuver

"The L-1 maneuver is similar to the M-1 maneuver except the aircrew *member forcefully attempts to exhale against a* completely closed glottis while tensing all skeletal muscles. Using either maneuver the pilot obtains equal protection, i.e. 1.5 G greater than relaxed blackout level with or without the anti-G suit. In a 1972 study, subjects wearing anti-G suits and performing either the M-1 or L-1 straining maneuver were able to maintain adequate vision during centrifuge exposure of +9 G for 45 seconds. Higher and longer runs have not been attempted. However, it is important to note (a word of caution) that forcefully exhaling against a closed glottis without vigorous skeletal muscular tensing (Valsalva maneuver) can reduce +G tolerance and lead to an episode of unconsciousness at extremely low G_z levels. Therefore, instruction and training on the proper method of performing these straining maneuvers is essential." (Source: Gillingham, K. K. and Krutz, USAFSAM AR 10-74, Brooks AFB, Texas 78235).

BIBLIOGRAPHY

1. Barton, R. F., A Primer on Simulation and Gaming, Englewood Cliffs, N.J.: Prentice Hall, 1970.

2. Berne, Robert M. and Levy, M. N., Cardiovascular Physiology, 2nd Ed., St. Louis, Missouri: The C. V. Mosby Company, 1972.

3. Bigland, B. and Lippold, O. C. J., "The Relation Between Force, Velocity and Integrated Electrical Activity in Human Muscles," J. Physiol., Vol. 123, 1954, pp. 214-224.

4. Brody, G., Scott, R. N., and Balasubiramanian, R., "A Model for Myoelectric Signal Generation," Medical and Biological Engineering, January 1974, pp. 29-41.

5. Burton, R. R., Leverett, S. D., and Michaelson, E. D., "Man at High Sustained +G_z Acceleration: A Review," Aerospace Med., Vol. 45, No. 10, 1974, pp. 1115-1136.

6. Cadzow, J. A. and Martens, H. R., Discrete-Time and Computer Control Systems, Edited by F. F. Kuo, Englewood Cliffs, N. J.: Prentice Hall, 1970.

7. Chambers, R. M. and Hitchcock, Lloyd, Effects of Acceleration on Pilot Performance, Johnsville, Penn.: U.S. Naval Air Development Center, NADC-MA-6219, March 1963.

8. Chambers, R. M., "Acceleration", Chapter 3, Bioastronautics Data Book, NASA SP 3006, 1964.

9. Clark, W. G. and Jorgenson, H., Studies of Self-Protective Anti-Blackout Maneuvers, Washington, D.C.: National Research Council, Committee on Aviation Medicine, Report No. 488, 1945.

10. Coggshall, J. C. and Bekey, G. A., "EMG-FORCE Dynamics in Human Skeletal Muscle," Medical and Biological Engineering, Vol. 8, No. 3, May 1970, pp. 265-270.

11. Cole, D. F., "Comparative Aspects of Intraocular Fluids," Chapter 2 in The Eye, Vol. 5, Davison, H. and Graham, L. T., Jr., N. Y.: Academic Press, 1974.

12. Davenport, Wilbur B., Jr. and Root, William L., Random Signals and Noise, N. Y.: McGraw Hill Book Co., 1958.

13. Davson, H., editor, The Eye, 2nd Ed., N.Y.: Academic Press, 1969.

14. Forrester, J. W., World Dynamics, Cambridge, Mass.: Wright Allen Press, Inc.

15. Fraser, T. M., Human Responses to Sustained Acceleration, NASA SP-103, 1966.

16. Gauer, O. H. and Zuidema, G. D., Gravitational Stress in Aerospace Medicine, Boston, Mass.: Little, Brown & Co., 1961.

17. Gauer, O. H., "The Physiological Effects of Prolonged Acceleration," in German Aviation Medicine, World War II, Vol. I, Washington, D. C.: Superintendent of Documents, U.S. Government Printing Office, 1950.

18. Gillingham, K. K. and McNaughton, G. B., "Visual Field Contraction During G Stress at 13°, 45° and 65° Seatback Angles," Aviation Space and Environmental Med., Vol. 48, No. 2, 1972, pp. 91-96.

19. Gillingham, K. K., Freeman, J. J., and McNee, R. C., "Transfer Functions for Eye Level Blood Pressure During +G_z Stress," Aviation Space and Environmental Med., Vol. 48, No. 11, 1972, pp. 1026-1034.

20. Gillingham, K. K. and Krutz, R. W., Brooks AFB, Texas, USAFSAM AR10-74.

21. Glaister, D. H., The Effects of Gravity and Acceleration on the Lung, England: Technivision Services, AGARDograph 133, 1970.

22. Gray, H., Anatomy, Descriptive and Surgical, Philadelphia, Penn.: Running Press, 1974.

23. Gray, S., III., Shaver, J. A., Kroetz, F. W., and Leonard, J. J., "Acute and Prolonged Effects of G Suit Inflation on Cardiovascular Dynamics," AMA Proceedings, Bal Harbor, Florida, 1968.

24. Greer, B. Y., Smedal, H. A., and Wingrove, R. C., Centrifuge Study of Pilot Tolerance to Acceleration and the Effects of Acceleration on Pilot Performance, NASA TN D-337, 1960.

25. Ham, G. C., "Effects of Centrifugal Acceleration on Living Organisms," War Med., Vol. 30, No. 3, 1943.

26. Hamilton, W. F., R. A. Woodbury, and H. T. Harper, Jr., Physiologic relationships between intrathoracic, intraspinal and arterial pressures. J. Am. Med. Assoc. 107: 853, 1936.

27. Harrison, L., III., "A Study to Investigate the Feasibility of Utilizing Electrical Potentials on the Surface of the Skin for Control Functions, Blue Bell, Penn.: Philco Corp., Report No. 2386, AD-619311 July 1964.

28. Holden, Frank M., Rogers, D. B., Evaluation of Arterial Oxygen Concentration in Human Exposed to G_z G_x Acceleration Forces. AMRL-TR-73-81, Nov. 1973.

29. Howard, P., "The Physiology of Positive Acceleration," Chapter 23 in A Textbook of Aviation Physiology, Edited by J. A. Gilles, Pergamon Press, 1965.

30. Knapp, C., Randall, D., Evans, J. and Marquis, J., "Frequency Response of Cardiovascular Regulation in Canines to Sinusoidal Acceleration at Frequencies Below 1.5 Hz," paper presented at the Review of Air Force

Sponsored Basic Research in Environmental and Acceleration Physiology, Wright-Patterson AFB, Ohio, October 13-15.

31. Knapp, C. F., Evans, J., and Randall, D., Cardiovascular Regulation During Low Frequency (<0.3 Hz) Sinusoidal Acceleration in Normal and Cardiac Denervated Dogs. Preprints of Aerospace Medical Association, May 1979, pp. 131-132.

32. Koushanpour, E. and Spickler, J., "Effect of Mean Pressure levels on the Dynamic Response Characteristics of the Carotid Sinus Baroreceptor Process in a Dog," IEEE Trans. Biomed. Engineering, BME, Vol. 22, No. 3, 1975, pp. 502-507.

33. Karon, G., Young, L., and Alberry, W., "High-G Simulation - The Tactical Aircraft Simulator Problem," Proceedings of the 10th NTEC/Industry Conference, Orlando, Florida, November 1977, pp. 49-59.

34. Lambert, E. H., "The Physiologic Basis of 'Blackcut' as It Occurs in Aviators," Fed. Proc., Vol. 4, 1945, p. 43.

35. Lambert, E. H., "Physiologic Studies of Man's G Tolerance in Aircraft," Fed. Proc., Vol. 5, 1946, p. 59.

36. Lambert, E. H., Wood, E. H., and Baldes, E. J., The Protection Against the Effects of Acceleration Afforded by Pulling Against a Weighted Control Stock and the Influence of this on the Effectiveness of Pneumatic Anti-Blackout Suits, Washington, D.C.: National Research Council, Committee on Aviation Medicine, Report No. 265, 1944.

37. Leverett, S. D., Whitney, R. U., and Zuidema, G. C., "Protective Devices Against Acceleration," in Gravitational Stress in Aerospace Medicine, Edited by O. H. Gauer and G. D. Zuidema, Boston, Mass.: Little, Brown & Co., 1961.

38. Levison, W., Barnett, G., and Jackson, W., "Nonlinear Analysis of the Baroreceptor Reflex System," Circulation Research, Vol. 18, 1966, pp. 673-682.

39. Lewis, D. H., "An Analysis of Some Current Methods of G Protection," J. Aviat. Med., Vol. 26, 1955, p. 479.

40. Lewis, D. H. and Duane, T. D., "Electroretinogram in Man During Blackout," J. Appl. Physiol., Vol. 9, 1956, p. 105.

41. Lind, A. R., Taylor, S. H., Humphreys, P. W., Kennelly, B. M. and Donald, K. W., "The Circulatory Effects of Sustained Voluntary Muscle Contraction," Clin. Sci., Vol. 27, 1964, p. 229.

42. Lind, A. R., McNicol, G. W., and Donald, K. W., "Circulatory Adjustments to Sustained (Static) Muscular Activity," Proc. Symp. Physical Activity in Health and Disease, Oslo: Universitetsforlaget, 1966, pp. 38-63.

43. Lindberg, E. F. and Wood, E. H., "Acceleration," in Physiology of Man in Space, Edited by J. H. U. Brown, N. Y.: Academic Press, 1963.

44. Lindberg, E. F., Sutterer, W. F., Marshall, H. W., Headley, R. N., and Wood, E. H., "Measurement of Cardiac Output During Headward Acceleration Using the Dye-Dilution Technique," Aerospace Med., Vol. 31, No. 8, 1960, p. 817.

45. Miller, N. C. and Green, J. F., "A Model Describing Acceleration-Induced Blackout," Annals of Biomedical Engineering, Vol. 2.

46. McCally, M., "The Effect of Sustained Muscular Contraction on Tolerance to $+G_z$ Acceleration," PhD Dissertation, The Ohio State University.

47. McRuer, D. T., Magdaleno, R. E., and Moore, G. P., "A Neuromuscular Actuation System Model: IEE Transactions on Man Machine Systems," MMS-0, No. 3, September 1968.

48. Newsom, W. A., Leverett, S. D., and Kirkland, V. E., "Retinal Circulation in Man During Centrifugal Acceleration," Trans. Amer. Acad. Ophthal. and Otalaryn., Vol. 72, 1968, p. 39.

49. Rushmer, R. F., "Circulatory Effects of Three Modifications of the Valsalva Experiment: An Experimental Survey," Amer. Heart J., 1946.

50. Scher, A. and Young, A., "Acceleration," in Physiology of Man in Space, Edited by J. Brown, N.Y.: Academic Press, 1963.

51. Shannon, R. E., Systems Simulatation: The Art and Science, Englewood Cliffs, N. J.: Prentice Hall, 1975.

52. Shwedyk, E., Balasubramanian, R., and Scott, R. N., "A Nonstationary Model for the Electromyogram," IEEE Transactions on Biomedical Engineering, Vol. BME-24, No. 5, 1977, pp. 417-424.

53. Stoll, Alice M., "Human Tolerance to Positive G as Determined by the Physiological End Points," Aviation Medicine, August 1956.

54. Wani, Ali M. and Guha, S. K., "Summation of Fibre Potentials and the e.m.g.-Force Relationship During the Voluntary Movement of a Forearm," Medical and Biological Engineering, March 1974, pp. 174-180.

55. Wiley, R. L. and Lind, A. R., "Respiratory Response to Sustained Muscle Contractions in Man," Fed. Proc., Vol. 29, 1970, p. 265.

56. Wirta, R. W., Cody, K. A., and Finley, F. R., "Myopotential Patterns and External Control: Effects of Practice and Fatigue, Willow Grove, Penna.: Philco Ford Corp., Report AD-655140, 1967.

57. White, William J., Acceleration and Vision, Wright-Patterson AFB, Ohio: Wright Air Development Center, WADC TR-58-333, November 1958.

58. Wood, E. H. and Lambert, E. H., "Some Factors Which Influence the Protections Afforded by Pneumatic Anti-G Suits," J. Aviat. Med., Vol.

23, 1952, p. 218.

59. Zarriello, J. J., Seale, L. M., and Norsworthy, M. E., "The Relationship Between Cardiovascular Response and Positive G Tolerance," Aviation Medicine, November 1958.

60. Bioastronautics Data Book, Edited by Paul Webb, NASA SP-3006, 1964.

*U.S.Government Printing Office: 1979 — 657-002/132